J. Fluid Mech. (1993), *vol.* 252, *pp.* 1–30
Copyright © Cambridge University Press

Wave packets, resonant interactions and soliton formation in inlet pipe flow

By IGOR V. SAVENKOV

Computer Center of the Academy of Sciences, 117 967 Vavilova, 40, Moscow, Russia, CIS

(Received 8 April 1992 and in revised form 21 December 1992)

The development of disturbances (two-dimensional non-linear and three-dimensional linear) in the entrance region of a circular pipe is studied in the limit of Reynolds number $R \to \infty$ in the framework of triple-deck theory. It is found that lower-branch axisymmetric disturbances can interact in the resonant manner. Numerical calculations show that a two-dimensional nonlinear wave packet grows much more rapidly than that in the boundary layer on a flat plate, producing a spike-like solution which seems to become singular at a finite time. Large-sized, short-scaled disturbances are also studied. In this case the development of axisymmetric disturbances is governed by single one-dimensional equation in the form of the Korteweg–de Vries and Benjamin–Ono equations in the long- and short-wave limits respectively. The nonlinear interactions of these disturbances lead to the formation of solitons which can run both upstream and downstream. Linear three-dimensional wave packets are also calculated.

1. Introduction

The study of the instability of inlet pipe flow has occupied many researchers for the past several decades. This interest is excited by the fact that linear stability analysis of fully developed Hagen–Poiseuille flow predicts that it is stable whereas regions of fully developed turbulent flow were observed by Reynolds as far back as 1883. Therefore it was supposed that the observed instability is connected with the instability of a boundary layer which exist long before the pipe flow becomes fully developed. The linear analysis of Tatsumi (1952) and Huang & Chen (1974) has demonstrated such a possibility, and experiments by Wygnanski & Champagne (1973) and Sarpkaya (1975) confirmed this suggestion. It was found that instability waves, originating in a boundary layer, may burst into a turbulent spot. As the spot travels downstream it may increase in size until its dimension becomes comparable with the radius of the pipe. As a result a turbulent slug appears, temporarily filling the entire cross-section of the pipe with a turbulent flow. (It should be remarked that another type of turbulent flow can exist, namely puffs which are generated by larger disturbances at the inlet; both disturbance types can be observed long before the flow becomes fully developed.)

Another possible explanation of circular pipe flow instability is that laminar–turbulent transition may be initiated by disturbances, whose size, although small, is sufficiently large relative to the inverse powers of Reynolds number that the stability properties of the basic flow are altered significantly, by a relative amount of $O(1)$, from the classical linear properties. Such a rational high-Reynolds-number analysis was done by Smith & Bodonyi (1980) in the context of a fully nonlinear critical layer. Their suggestions on the so-called Rayleigh stage of nonlinear amplitude-dependent instability gave rise to the theory by Smith, Doorly & Rothmayer (1990), where an

attempt was made to give a unified theoretical description of spots in channels, pipes and boundary layers as well.

In the present study another high-Reynolds-number approach is developed, namely that based on the triple-deck theory of Stewartson (1969), Neiland (1969) and Messiter (1970). But the present study does not contradict the concept of Smith *et al.* (1990) and in fact may be regarded as complementary to theirs.

The triple-deck approach to the problem of the high-Reynolds-number instability has been intensively developed over the last ten years. The studying was initiated in papers by Smith (1979) and Zhuk & Ryzhov (1980), where it was shown that lower-branch Tollmien–Schlichting waves can be described in the framework of the triple-deck theory. Smith (1976) first applied triple-deck theory to stationary problems of inlet flows (in pipes and channels). Instability problems of entry flows then were studied by Smith & Bodonyi (1980), Bogdanova (1982) and Bogdanova & Ryzhov (1983). However, these studies were restricted to the analysis of normal modes with particular attention to linear neutral waves. But as a rule the most unstable waves play a dominant part in the linear instability process. So an extensive analysis of the dispersion relation is needed and it is given below in §3.2. It provides an explanation for particular features of the three-dimensional linear wave packets presented in §3.3. The subsequent nonlinear stage of wave-packet development is investigated in §4, but only for axisymmetric disturbances.

Linear analysis predicts the possibility of resonant interactions on purely axisymmetric (i.e. effectively two-dimensional) disturbances. The computations of §4.1 show that resonant interactions do take place for dimensionless pipe radius $r_0 \leqslant 1$. They lead to the enhanced growth of disturbances, producing a sharp spike, so the possible breakdown of the governing equations occurs sooner than that in the case of two-dimensional disturbances in the boundary layer on a flat plate (see Duck 1985, 1987; Ryzhov & Savenkov 1989, 1992 and §4.1.1) when non-resonant amplification takes place. In the boundary layer on a flat plate resonant interactions may and do occur, but only on three-dimensional waves. These interactions play a key (or at least important) role in most cases of laminar–turbulent transition (Kachanov & Levchenko 1982, 1984; Kachanov 1987, 1991*a*) and references therein).

A theoretical investigation of resonant-triad interactions was put forward by Craik (1971), who proposed that a two-dimensional Tollmien–Schlichting (TS) wave could interact nonlinearly with two oblique three-dimensionsl TS waves, in such a way that the nonlinear interplay reinforces all three waves. Resonant interactions were studied on the basis of a rational high-Reynolds-numbers approach by Smith & Stewart (1987) (a finite-amplitude/relatively high-frequency approach) and Goldstein & Leib (1989), Goldstein & Choi (1989) (the effect of critical-layer nonlinearity on oblique instability waves on shear layers). Thus a specific feature of inlet flows (not only pipe, but channel flows as well; see Savenkov 1992) is that powerful resonant interactions are possible even on two-dimensional disturbances.

Further computations show that with the decrease of pipe radius r_0 the maximum growth rate falls and the spike formation process is prolonged (§4.1.3). A high-frequency/large-amplitude analysis in the limit as $r_0 \to 0$ (§4.2) leads to an inviscid problem which for a boundary layer on a flat plate was first formulated by Zhuk & Ryzhov (1982) and Smith & Burggraf (1985). In the latter case this inviscid problem reduces to the well-known Benjamin–Ono equation having solutions in forms of solitons. The renewed interest in the Benjamin–Ono equation (in the context of laminar–turbulent transition) in Rothmayer & Smith (1987) and Ryzhov (1990) is associated with experimental observations of soliton-like structures (Borodulin &

Kachanov 1990; Kachanov 1991 *a*, *b*) in the *K*-regime of boundary-layer transition. So §5 is devoted to the investigation of an inviscid problem obtained for the inlet pipe flow. (This problem can also be derived from the original system of Navier–Stokes equations.) This problem also admits solitons, which are studied in §5.2. It is shown that in two extreme limits – long-wave and short-scale ones – the problem reduces to the classical Korteweg–de Vries and Benjamin–Ono equations respectively. In the general case solitons are calculated by use of a pseudo-spectral scheme. They can run both upstream and downstream. In §5.3 a receptivity problem is considered, i.e. the problem of how solitons are produced by external sources.

2. Problem formulation

We shall consider the entrance region of a circular pipe flow at high Reynolds numbers. The boundary layer emanating from the leading edge of the pipe wall 'fills' the pipe only very far from the inlet. So at high Reynolds numbers there is a vast region of developing flow, the instability of which will be considered here following Smith & Bodonyi (1980), Bogdanova & Ryzhov (1983) and Bogdanova (1982).

Following Smith (1976) we consider disturbances at the distance $L^* \sim b_0^* R_L^{\frac{1}{8}} \Delta$ from the entrance (the local Reynolds number $R_L = U_\infty^* L^*/\nu_\infty^*$ is based on the length L^*; U_∞^* is the free-stream speed of the oncoming uniform flow, ν_∞^* is the kinematic viscosity and ρ_∞^* is the density; the small parameter $R_L^{-\frac{1}{8}} \ll \Delta \ll 1$). Hence the pipe radius b_0^* is of the order of the lengthscale $b^* \sim L^* R_L^{-\frac{1}{2}} \Delta^{-1}$ of the interaction zone in the triple-deck structure of Stewartson (1969), Neiland (1969) and Messiter (1970).

We shall use a non-dimensional system of units, with velocity components (u, v, w), cylindrical coordinates (x, r, θ), excess pressure p and time $\bar{t}$ being non-dimensionalized with respect to U_∞^*, b^*, $\rho^* U_\infty^{*2}$ and b^*/U_∞^* respectively. Finally we define $R = U_\infty^* b^*/\nu_\infty^*$ and set $R \to \infty$.

In the lower deck, which is of primary concern in the triple-deck theory, we put (Smith 1976; Smith & Bodonyi 1980; Bogdanova 1982)

$$(u, v, w, p) = (\Delta U, -\Delta^3 V, \Delta W, \Delta^2 P) + \ldots, \tag{2.1a}$$

with time–space variables

$$(\bar{t}, x, y, \theta) = (\Delta^{-1} t, \Delta^2 R + X, r_0 - \Delta^2 Y, \theta) + \ldots, \tag{2.1b}$$

where the non-dimensional pipe radius $r_0 = b_0^*/b^*$.

The governing equations in this deck are then

$$\frac{\partial U}{\partial X} + \frac{\partial V}{\partial Y} + \frac{\partial W}{\partial \theta} = 0; \quad \frac{\partial P}{\partial Y} = 0, \tag{2.2a, b}$$

$$\frac{\partial U}{\partial t} + U\frac{\partial U}{\partial X} + V\frac{\partial U}{\partial Y} + W\frac{1}{r_0}\frac{\partial U}{\partial \theta} = -\frac{\partial P}{\partial X} + \Delta^{-5} R^{-1} \frac{\partial^2 U}{\partial Y^2}, \tag{2.2c}$$

$$\frac{\partial W}{\partial t} + U\frac{\partial W}{\partial X} + V\frac{\partial W}{\partial Y} + W\frac{1}{r_0}\frac{\partial W}{\partial \theta} = -\frac{1}{r_0}\frac{\partial P}{\partial \theta} + \Delta^{-5} R^{-1} \frac{\partial^2 W}{\partial Y^2}. \tag{2.2d}$$

For $\Delta = R^{-\frac{1}{5}}$ this system coincides with the system of Prandtl equations, but now the pressure P is self-induced and unknown. This pressure is produced by means of the interaction of the lower deck with the outer region of an inviscid irrotational flow. The flow in the outer region turns out to be governed by the Prandtl–Glauert equation, solution of which may be symbolically written as

$$P = \mathscr{L}(A) \tag{2.3a}$$

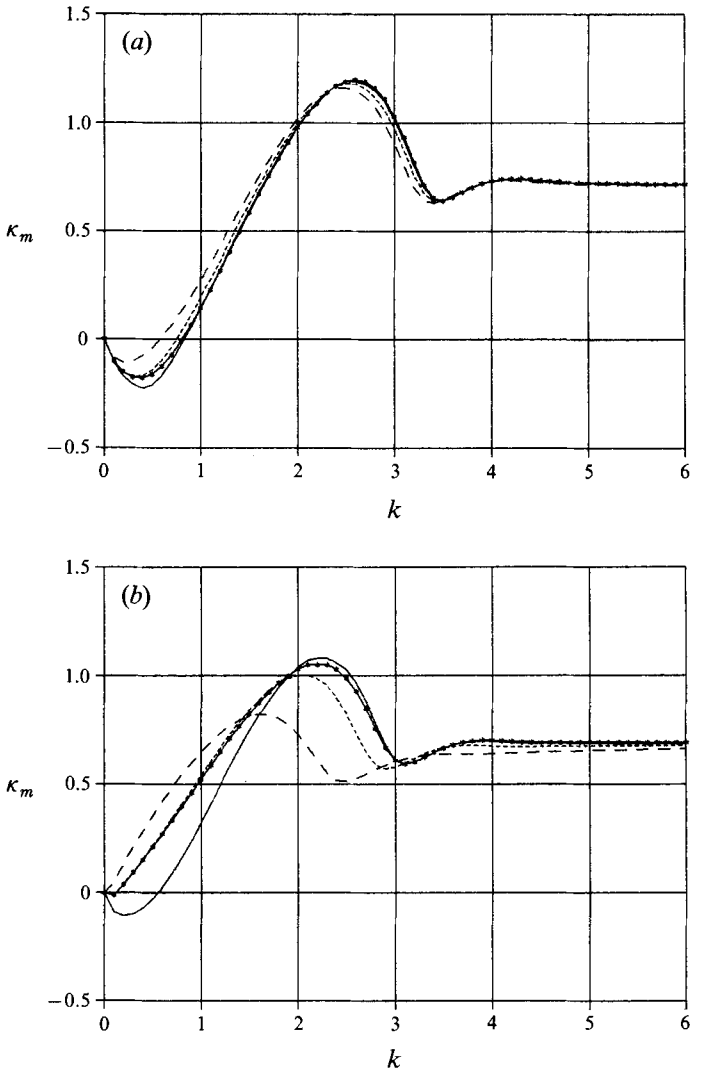

FIGURE 1 (*a*, *b*). For caption see facing page.

where the linear operator $\mathscr{L}$ is defined by its spectrum λ (see, for example, Smith 1976; Bogdanova 1982):

$$\mathscr{L}(E) = \lambda E, \quad E = \exp(\mathrm{i}kX + \mathrm{i}m\theta), \tag{2.3b}$$

$$\lambda_m(k) = kI_m(kr_0)/I'_m(kr_0), \tag{2.3c}$$

where $I_m(z)$ is modified Bessel function of the first kind and mth order.

Here the displacement function $A(t, X, \theta)$ arises from consideration of flow in the main deck coinciding with the basic boundary layer. To close the problem we must set matching conditions

$$U - Y \to A, \quad W \to 0 \quad \text{as} \quad Y \to \infty \tag{2.4}$$

and wall conditions which depend on the particular situation.

Further formulation of the problem depends on the relation between Δ and $R^{-\frac{1}{5}}$. For this reason the cases $\Delta \sim R^{-\frac{1}{5}}$ and $\Delta \gg R^{-\frac{1}{5}}$ will next be considered separately.

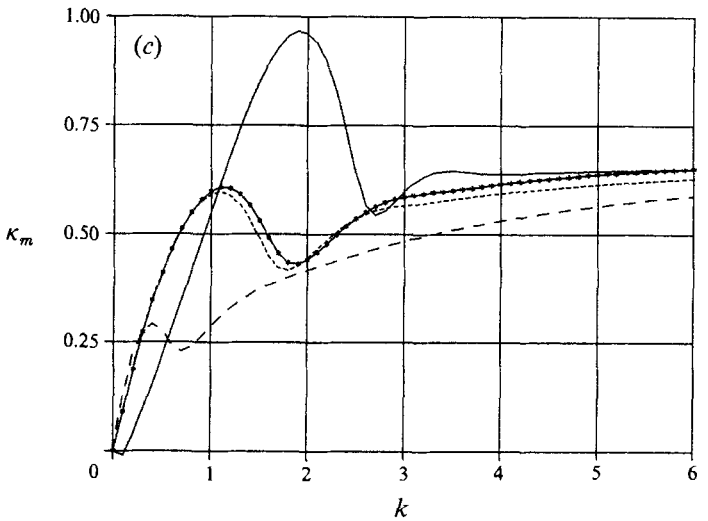

FIGURE 1. Growth rates κ_m for first modes: *−*−*−*, axisymmetric ($m = 0$); ——, first non-axisymmetric ($m = 1$); ----, second non-axisymmetric ($m = 2$); – – – –, third non-axisymmetric ($m = 3$); at various values of non-dimensional radius r_0: (*a*) $r_0 = 3$; (*b*) $r_0 = 1$; (*c*) $r_0 = \frac{1}{2}$.

3. Linear three-dimensional wave packets

3.1. *Dispersion relation*

The case $\Delta \sim R^{-\frac{1}{5}}$ corresponds to lower-branch instability, first studied by Smith & Bodonyi (1980) and later by Bogdanova (1982) and Bogdanova & Ryzhov (1983). They investigated small free flow oscillations of the kind

$$(U-Y, V, W, P, A) = \delta(\bar{U}, \bar{V}, \bar{W}, \bar{P}, \bar{A}) \exp(\omega t + \mathrm{i}kX + \mathrm{i}m\theta) \tag{3.1}$$

with no-slip ensured at the wall

$$U = V = W = 0 \quad \text{at} \quad Y = 0. \tag{3.2}$$

Then after setting the amplitude parameter $\delta \to 0$ we arrive at a linearized problem. This problem is an eigenvalue one and its solution leads to the dispersion relation (Smith & Bodonyi 1980; Bogdanova 1982)

$$\Phi(\Omega) = Q_m(k), \quad \Omega = \omega(\mathrm{i}k)^{-\frac{2}{3}}, \tag{3.3a}$$

$$\Phi = \frac{\mathrm{dAi}(\Omega)}{\mathrm{d}\zeta} I^{-1}(\Omega), \quad I = \int_{\Omega}^{\infty} \mathrm{Ai}(\zeta)\,\mathrm{d}\zeta, \tag{3.3b}$$

$$Q_m = (\mathrm{i}k)^{\frac{1}{3}} k \frac{I_m(kr_0)}{I'_m(kr_0)}\left[1 + \frac{m^2}{(kr_0)^2}\right], \tag{3.3c}$$

where $\mathrm{Ai}(\zeta)$ is the Airy function decaying exponentially in the sector $|\arg\zeta| < \frac{1}{3}\pi$. In (3.3) m must be an integer, whereas either the wavenumber k or the frequency $\omega_0 = -\mathrm{i}\omega$ may be a parameter taking on real values. It is well known that dispersion relations of the kind (3.3*a*) have the numerable set of roots (for each m) $\omega_n = (\mathrm{i}k)^{\frac{2}{3}}\Omega_n(k;m)$ originated at $k = 0$ from zeros of the Airy function derivative. Only one of these roots, namely the first, is unstable, i.e. $\mathrm{Re}\,\omega_1 > 0$ for some values of k, m.

Smith & Bodonyi (1980) and Bogdanova (1982) studied only neutral stability, when $\mathrm{Im}\,\omega_0 = \mathrm{Im}\,k = 0$. But it is well known that most unstable waves are of primary importance in developing the linear instability process. So we should proceed further in studying the dispersion relation (3.3).

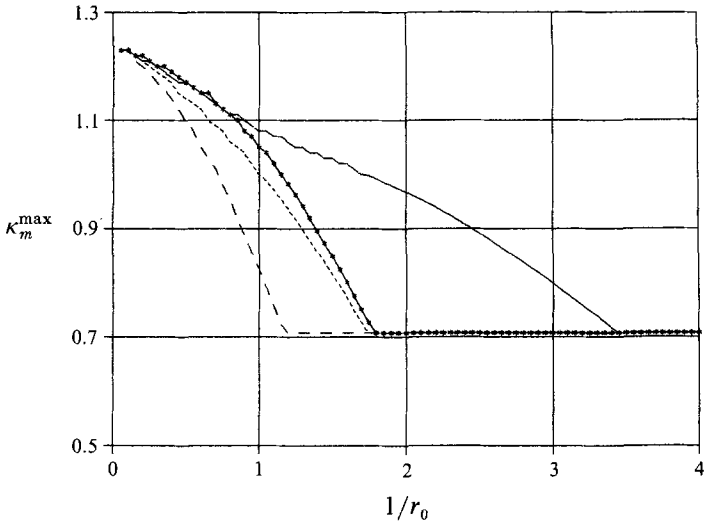

FIGURE 2. Maximum growth rate κ_m for first modes (curves as on figure 1) versus $1/r_0$.

3.2. *Further study of the dispersion relation*

We will be interested in the so-called temporal instability, setting k to be a real parameter and searching for complex values of ω by numerical solving of (3.3). In (3.3) the non-dimensional radius r_0 is a parameter which is related to the non-dimensional distance from the pipe entrance by $r_0 \sim L^{-\frac{5}{8}}$ (see Smith 1976).

First, consider the flow near the inlet (small L or large r_0) and then decrease the value of r_0, corresponding to a downstream movement into the pipe (increasing L). As $r_0 \to \infty$ and $k, m = O(1)$, $Q_m \to Q_{\mathrm{BL}}(k, m=0) = (\mathrm{i}k)^{\frac{1}{3}}|k|$, i.e. the Blasius stability properties are retrieved, as one would hope, nearer the pipe entrance (Smith & Bodonyi 1980). This large-r_0 approximation is good enough even for $r_0 = 3$, see figure 1 (*a*). This figure shows that first several modes have practically identical dispersion properties (wave dispersion in the azimuthal direction appears only at $m \sim r_0$), so corresponding curves (on figure 1 *a*) differ only slightly from that of the boundary layer on a flat plate. Let us define the maximum growth rate $\kappa_m^{\max} = \max \mathrm{Re}\,\omega_1(k; m) = \mathrm{Re}\,\omega_1(k_m^{\max}; m)$ and next trace its dependence on r_0. Results are summarized in figure 2. With increasing r_0 the maximum growth rate goes down and the first non-axisymmetric mode is the most slow decaying. Therefore it becomes the most unstable (at $r_0 \approx 1$) whereas the axisymmetric mode approaches the second non-axisymmetric one (more details are shown in figure 1 *b*). So at $r_0 = \frac{1}{2}$ the first non-axisymmetric mode has approximately two-fold domination in comparison with the axisymmetric one (see also figure 1 *c*). Finally at $r_0 \approx 0.3$ the value of $\kappa_m^{\max}$ falls to its asymptotic value of $\frac{1}{2}\sqrt{2}$ (for all m) in accordance with the short-wave asymptote

$$\omega_1 = -\mathrm{i}k^2 + (1-\mathrm{i})\tfrac{1}{2}\sqrt{2} + \ldots \quad \text{as} \quad k \to +\infty,$$

which is just the same as for triple-deck disturbances in the boundary layer on a flat plate (see, for example, Smith 1986; Ryzhov & Terent'ev 1986). The asymptotic value $\frac{1}{2}\sqrt{2}$ corresponds to high-frequency waves (see also figure 1), so one can conclude that far downstream from the inlet relatively high-frequency waves may become more important and start to play the leading role in the instability process. The second general conclusion concerns the importance of the first non-axisymmetric mode. (It is interesting to note that wavenumbers $m = \pm 1$ were emphasized by Smith & Bodonyi

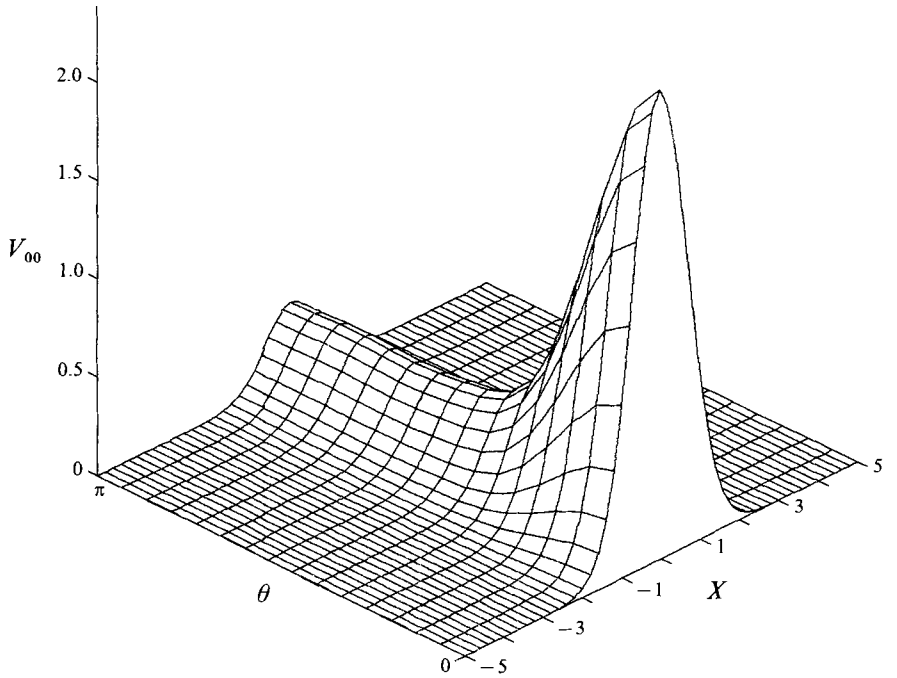

FIGURE 3. Source function $V_{00}(X, \theta)$.

1982 in their study of the nonlinear instability of a fully developed Hagen–Poiseuille flow.) How its predomination is revealed is the subject under consideration in the next subsection.

3.3. *Wave packets*

One part of the whole hydrodynamics stability problem is the problem of receptivity, i.e. how various external disturbances excite free flow oscillations. In the context of triple-deck theory this problem has been intensively studied in the last few years (see reviews of Ryzhov & Savenkov 1989; Goldstein & Hultgren 1989; Kozlov & Ryzhov 1990 and references therein). Its investigation requires solving the initial-value problem which, for the case of blowing–suction as an external source considered below, consists of equations (2.2)–(2.4) with the wall conditions

$$U = W = 0, \quad V = \delta V_0(t, X, \theta) \quad \text{at} \quad Y = 0. \tag{3.4}$$

Next we shall consider the linear receptivity problem assuming $\delta \to 0$. Using Fourier–Laplace transformation leads to the formula for perturbed wall shear $\tau'_w = \partial U/\partial Y - 1$ (Ryzhov & Savenkov 1989)

$$\tau'_w = 4\,\mathrm{Re}\left(\int_0^\infty F(t,k) \exp(\mathrm{i}kX)\,\mathrm{d}k \right), \tag{3.5a}$$

$$F = \sum_{m=0}^{m=\infty} \cos(m\theta) \sum_{n=1}^{n=\infty} \frac{\mathrm{Ai}(\Omega_n)(\mathrm{i}k)^{\frac{1}{3}} \bar{V}_0(\omega_n, k, m)}{I(\Omega_n)\,\mathrm{d}\Phi(\Omega_n)/\mathrm{d}\Omega} \mathrm{e}^{\omega_n t} + F_0, \tag{3.5b}$$

where F_0 is the term connected with the peculiarities (if any) of the function $\bar{V}_0(\omega, k, m)$ in the complex plane ω; and $\bar{V}_0$ stands for the Fourier–Laplace image

$$\bar{V}_0 = \frac{1}{4\pi^2} \int_{-\infty}^{\infty} \mathrm{d}x \int_{-\pi}^{\pi} \mathrm{d}\theta \int_0^\infty V_0(t, X, \theta) \exp(-\omega t - \mathrm{i}kX - \mathrm{i}m\theta)\,\mathrm{d}t. \tag{3.6}$$

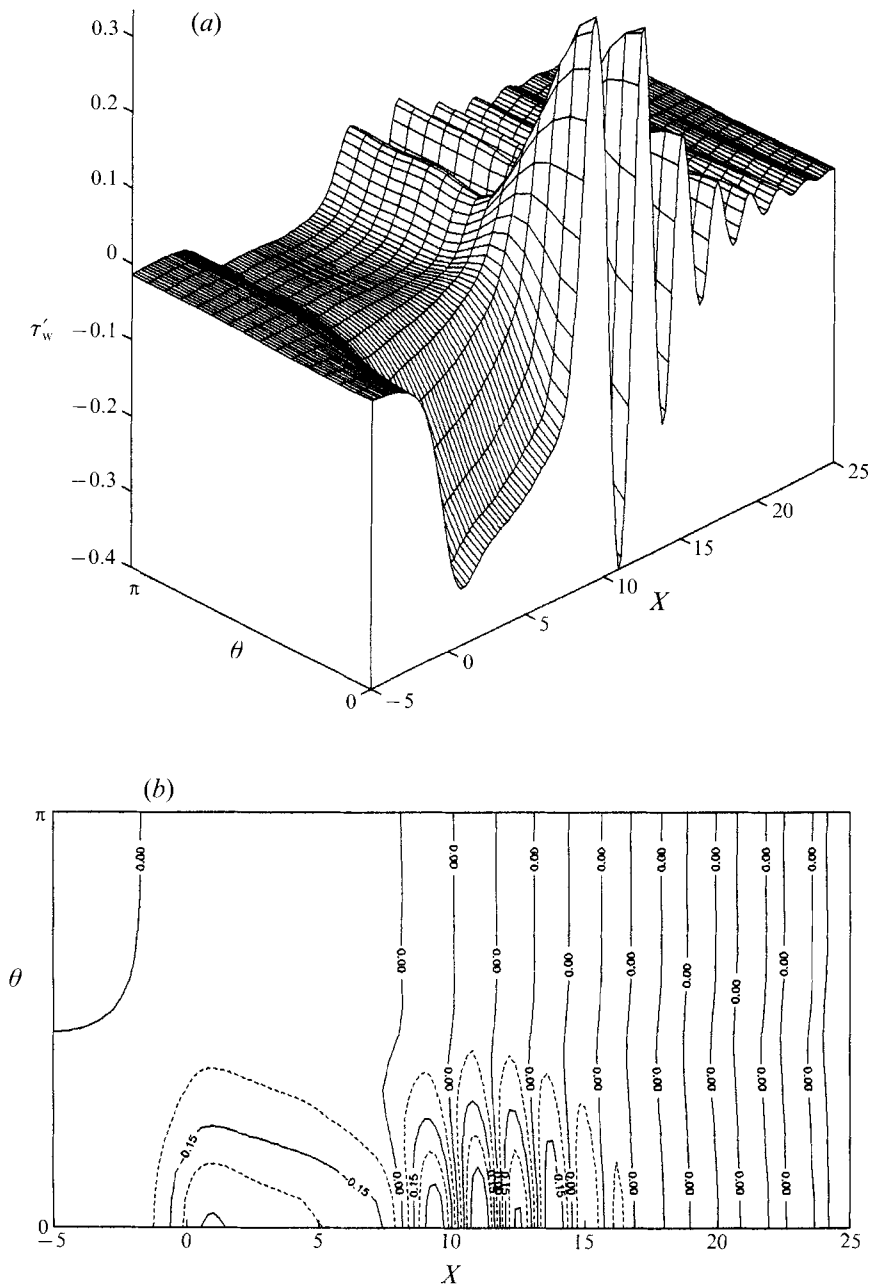

FIGURE 4. Three-dimensional linear wave packet at $r_0 = 3$ (at time $t = 3$): (*a*) perspective view; (*b*) disturbed surface stress τ'_w contours.

Consider next a pulse source ($|V_0| \to 0$ as $t \to \infty$) which excites a continuous k-spectrum of flow oscillations. Taking the source function V_0 of the form

$$V_0 = h(t) f(X) g(\theta) \quad \text{with} \quad h = Ht \exp(-t) \tag{3.7}$$

we set $H = 2$ and $f = \exp(-X^2)$ in all further computations. Choosing

$$g_m = \exp(-m^2/8)(8\pi)^{-\frac{1}{2}}$$

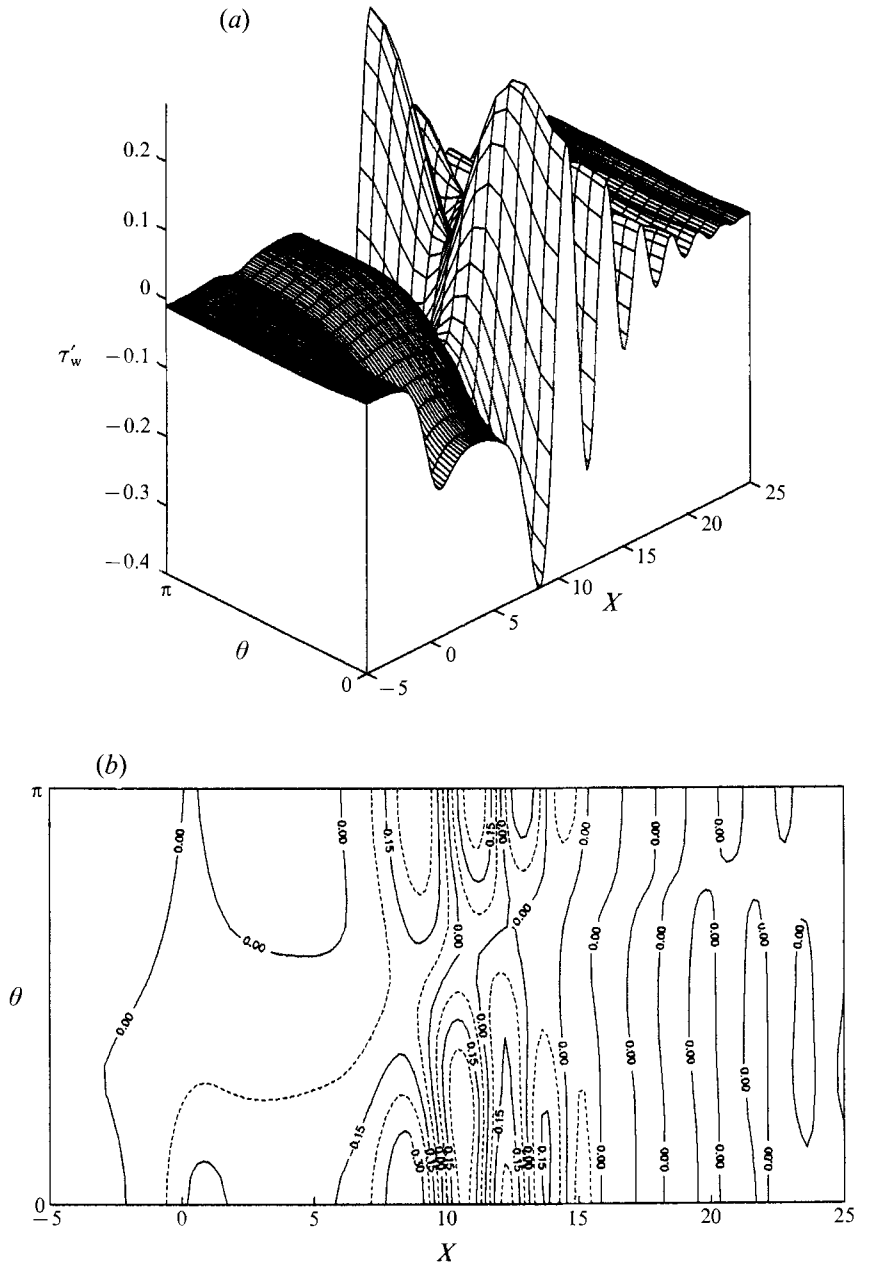

FIGURE 5. Same as figure 4 but for $r_0 = 1$.

we have a g-distribution such as presented in figure 3 (instead of $g = g_0(\theta) = \exp(-2\theta^2)$ for the case when $\bar{g}_m$ is defined by the integral transform).

The first pattern (figure 4) is for the case $r_0 = 3$ which corresponds to the immediate vicinity of the pipe entrance. In this case modes do not have any dispersion in the azimuthal direction. Therefore a wave packet at $r_0 = 3$ reproduces the θ-distribution of the g-function, so wave fronts are flat.

At $r_0 = 1$ (see figure 5) the first non-axisymmetric mode becomes dominant: the θ-distributions reveal a 'two-crest' shape for $10 < X < 15$. In the region $X > 15$ wave

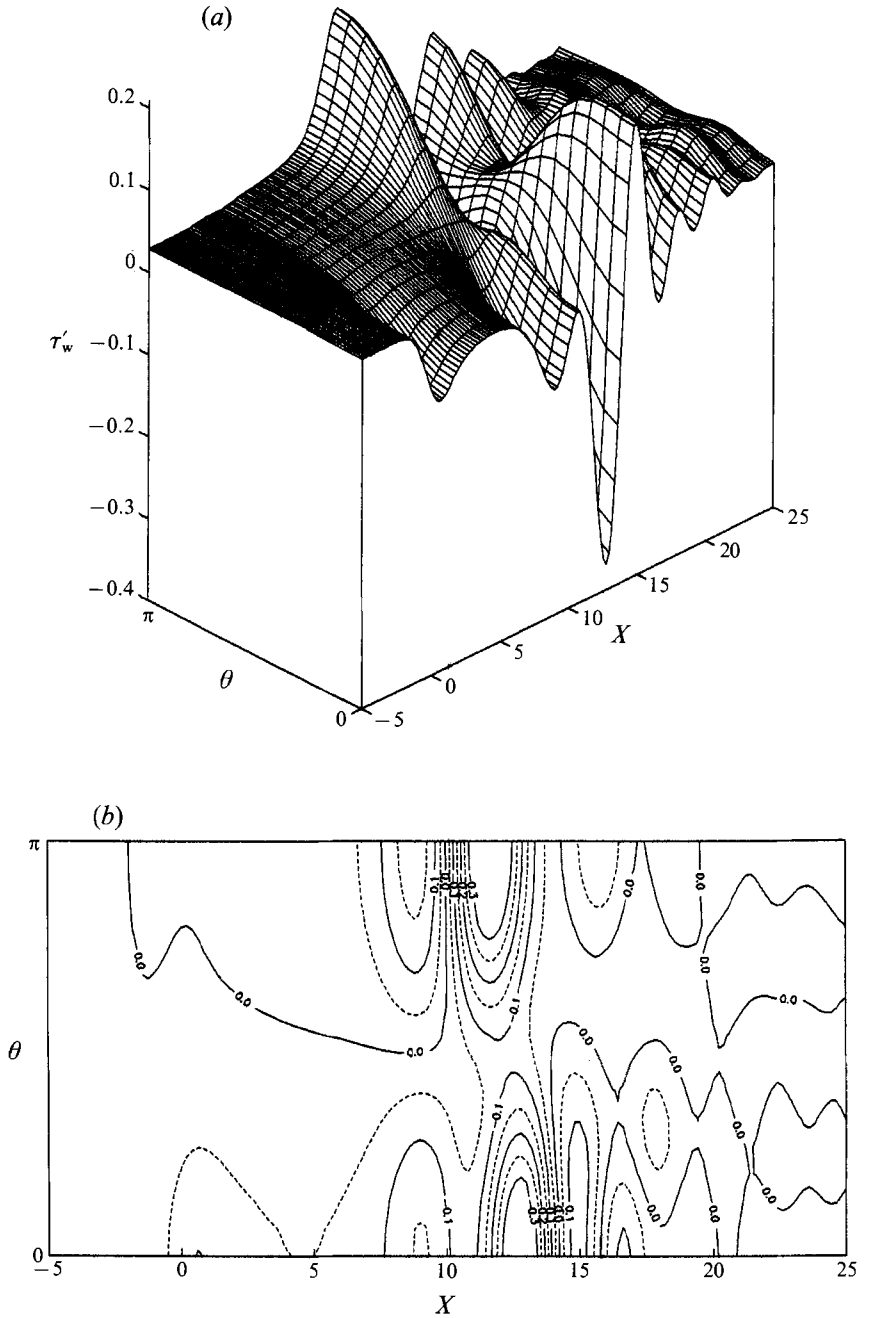

FIGURE 6. Same as figure 4 but for $r_0 = \frac{1}{2}$.

fronts remain flat due to over-riding of the axisymmetric mode there. Thus as early as at $t = 3$ the disturbances initially localized at $|\theta| < 1$ reach the opposite side of the pipe wall.

At $r_0 = \frac{1}{2}$ the first non-axisymmetric mode prevails over others that are reflected in θ-distributions (figure 6). Thus the non-axisymmetry of the flow may yet be revealed at the linear stage.

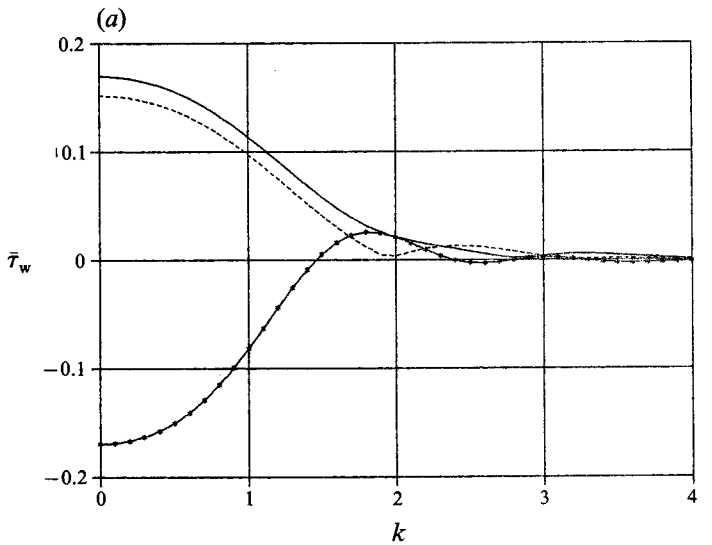

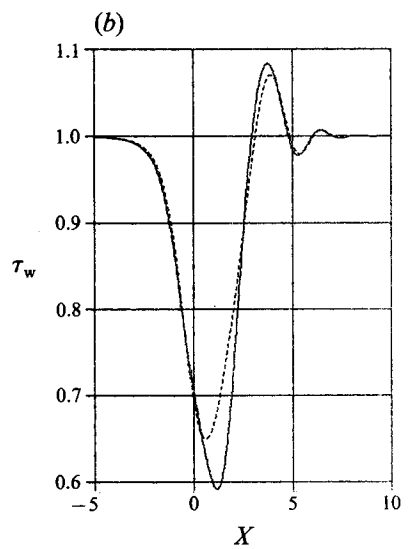

FIGURE 7. (*a*) Spectral distributions at $t = 1$ ($r_0 = 3$): $*-*-*-$, Re $\bar{\tau}_w(k)$; ——, amplitude $|\bar{\tau}_w|$; ----, $|\bar{\tau}_w|$ for linear case. (*b*) Surface stress $\tau_w(X)$ at $t = 1$ ($r_0 = 3$: ——, fully nonlinear; ----, linear case).

4. Nonlinear stage of development of axisymmetric disturbances

4.1. *Numerical results*

We shall solve the fully nonlinear problem (2.2)–(2.4), (3.4) with the use of the pseudo-spectral scheme of Burggraf & Duck (1981), developed later by Duck (1985, 1987, 1990), and restrict ourselves to a purely axisymmetric case. The pseudo-spectral method is based on the idea of decomposition of the solution into Fourier series (of the form $f(t, y)\exp(ikX)$, i.e. on the idea that is inherent in the normal-mode approach. So this method is efficient in solving linear and weakly nonlinear problems (in treating fully nonlinear ones it seldom if ever produces results better than those from other

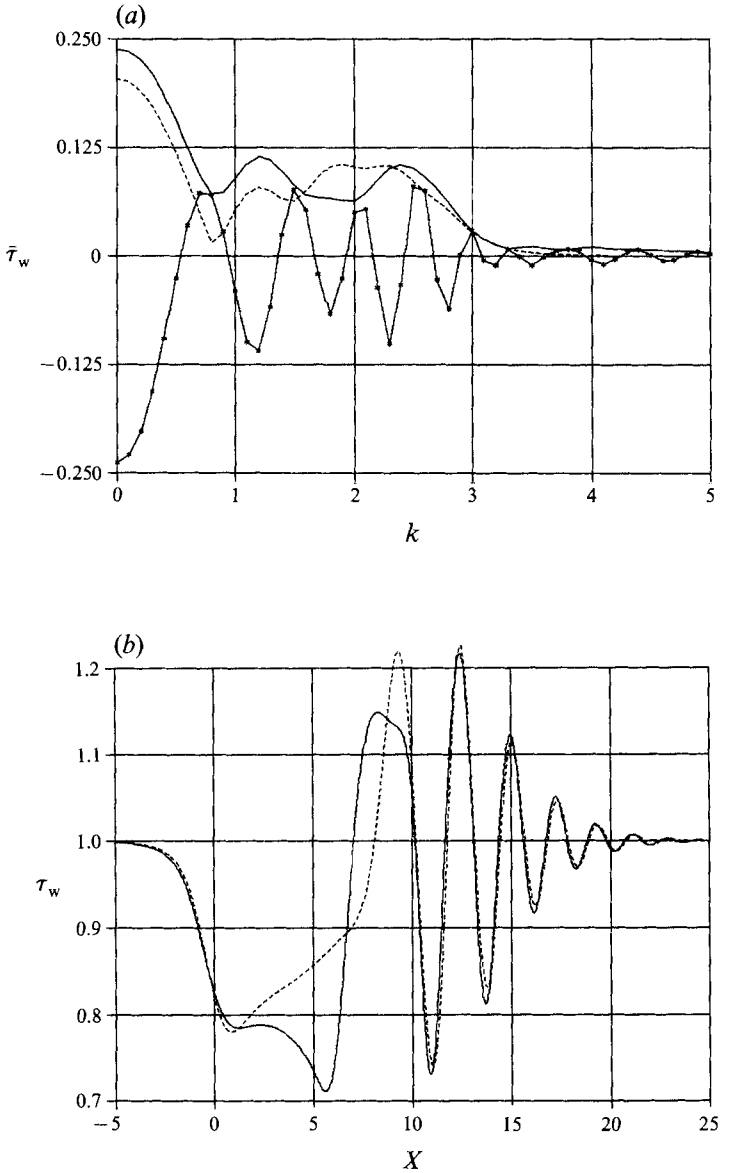

FIGURE 8. Same as figure 7 but at $t = 3$.

methods). Besides, in the Fourier space the interaction law (2.3*a*) takes its simple form (2.3*b*, *c*) and flow reversal is handled correctly without the need for any special treatment.

Throughout, in further computations 256 Fourier components were chosen with step $\Delta k = 0.1$ and 16 grid points were taken in the transformed (accordingly to $Y = \eta/(1-\eta)$) normal direction; timestep $\Delta t = 0.01$. The blowing-suction function V_0 is chosen in the form of (3.7) with $g(\theta) \equiv 1$, that is

$$V_0 = Ht\exp(-t-X^2). \tag{4.1}$$

Next we set $H = 2$ and will solve the problem for a number of values of $r_0 = 3$, 1, and $\frac{1}{4}$, corresponding to different distances from the pipe entrance.

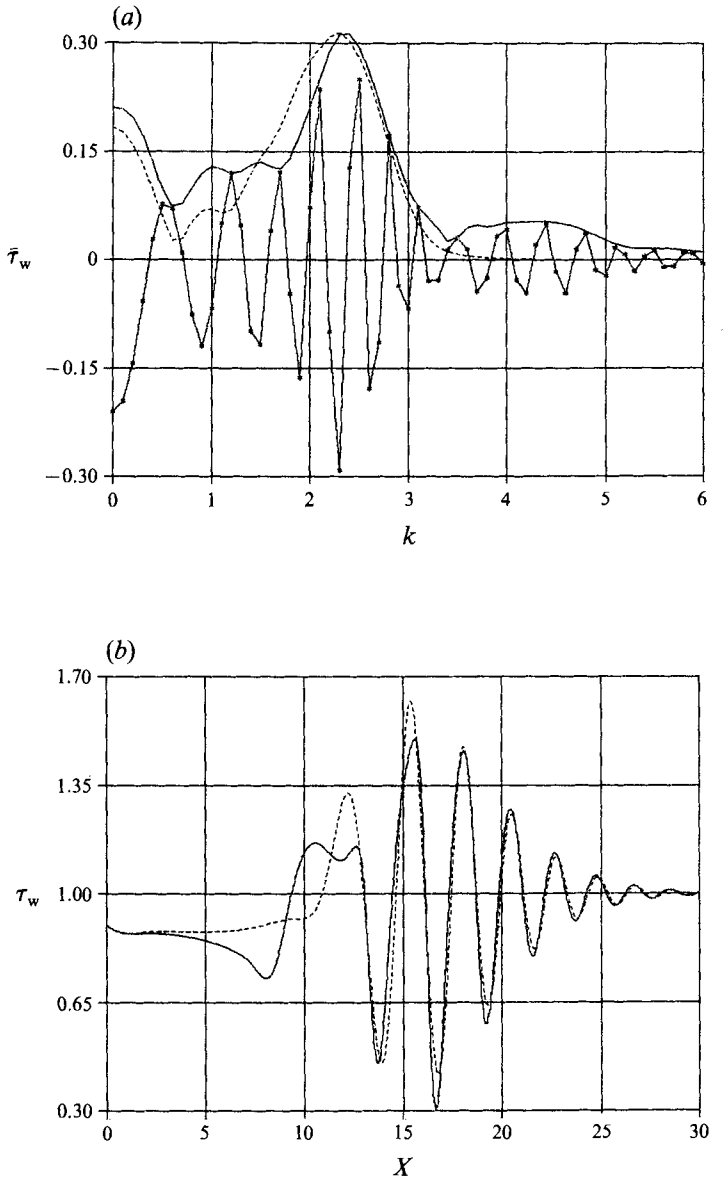

FIGURE 9. Same as figure 7 but at $t = 4$.

4.1.1. *Immediate vicinity of the pipe entrance* ($r_0 = 3$)

Since Blasius stability properties are retrieved in the immediate vicinity of the pipe entrance (Smith & Bodonyi 1980 and §3.2 above), one would expect that the scenario of disturbance development at $r_0 = 3$ resembles that for the boundary layer on a flat plate (as described by Duck 1987, 1990; Ryzhov & Savenkov 1989, 1992).

At small times up to $t = 1$ (figure 7) numerical solution is in accordance with the estimation

$$\tau'_w \sim -t^{\frac{3}{2}} V_{00}(X) \quad \text{as} \quad t \to 0+,$$

showing that the initial spectrum distribution is close to the function $\bar{V}_{00}(k)$. Nonlinearity has practically no effect on the solution at $t = 1$: the amplitude $|\bar{\tau}_w|$ grows

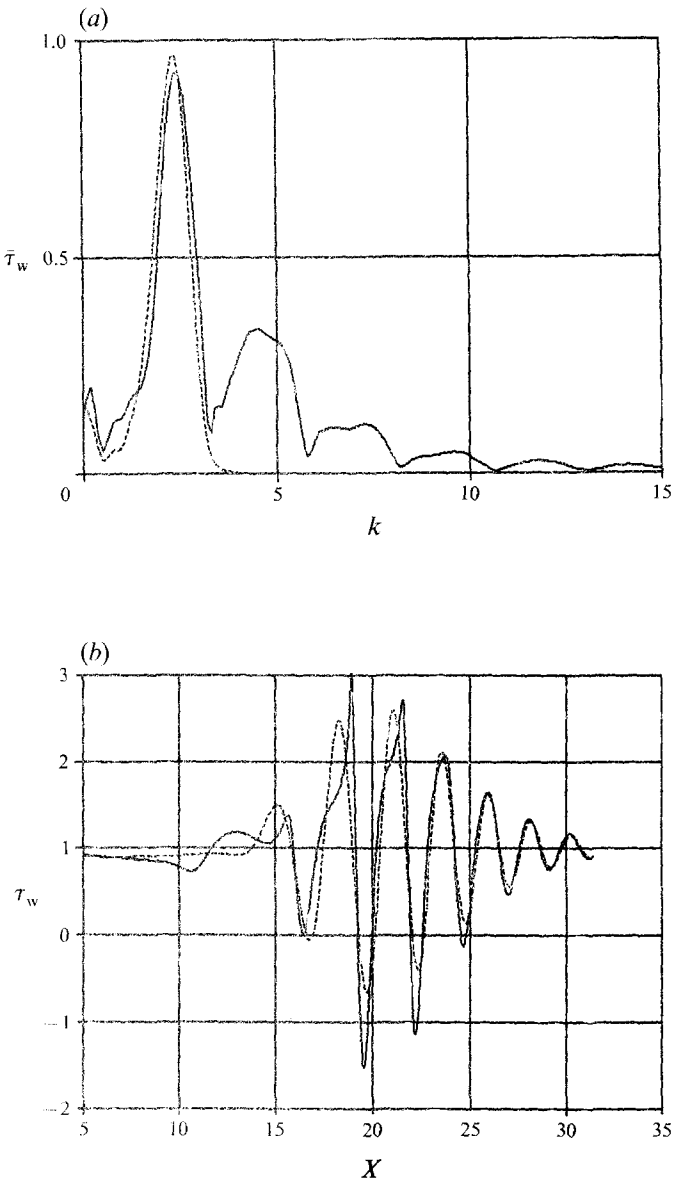

FIGURE 10. Same as figure 7 but at $t = 5$.

slightly in comparison with the linear case leading to some increase in amplitude of the negative peak $\tau'_w(X)$ (see figure 7). Moreover, even at $t = 3$ (figure 8) the nonlinear distortions may be seen only in the tail of the wave packet, whereas the main part of the wave packet which is formed from the most unstable waves remains almost the same as in the linear case. Finally at $t = 4$ the most unstable disturbances with wavenumbers k approaching $k_0^{\max} \approx 2.5$ take the leading role (figure 9) and reach amplitudes which are sufficient for nonlinear generation of the second harmonic. Nevertheless at this stage the second harmonic does not lead to any qualitative change in the solution (figure 9*a*). Later the generation of high-frequency harmonics with $k = nk_0^{\max}$ (and large n) takes place, which leads to gradual filling of the high-wavenumber spectra (figures 10 and 11 for $t = 5$ and 5.5 respectively). At the moment

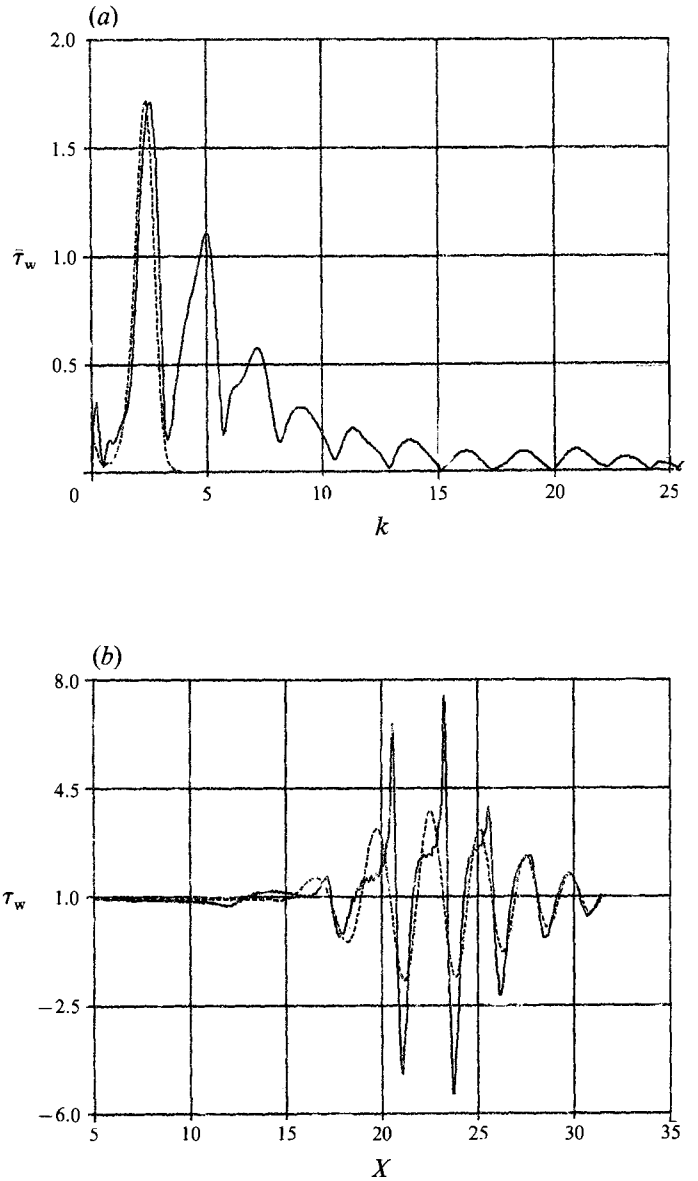

FIGURE 11. Same as figure 7 but at $t = 5.5$.

$t = 5.5$ disturbances reach the end of computational spectrum region ($k = 25.6$) and after this time the numerical scheme fails (with the chosen grid parameters).

The scenario of disturbance development is as follows: after the linear growth of the most unstable waves the second harmonic, the third one and so on are exited subsequently leading to amplification of peaks in the wave packet (figures 10 and 11) but not changing its group velocity. Note that even at the fully nonlinear stage the high harmonics do not affect in practice the first one with $k = k_0^{\max}$ (see comparison with the linear case in figures 10 and 11).

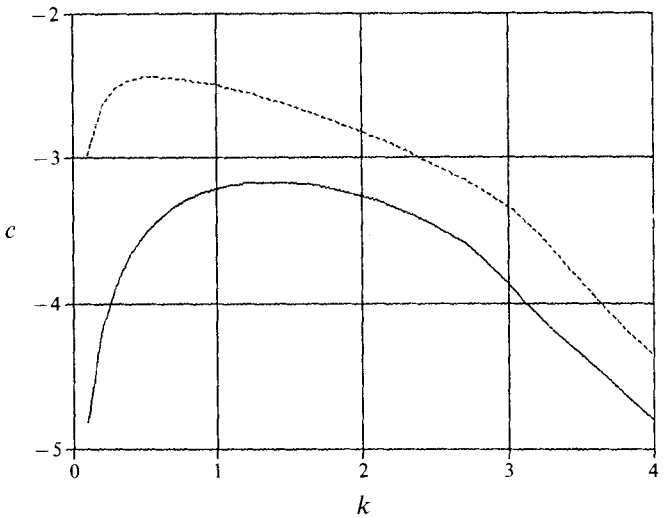

FIGURE 12. Phase velocity $c(k) = \mathrm{Im}\,\omega_1\,(k;0)/k$: ----, $r_0 = 3$; ——, $r_0 = 1$.

4.1.2. *Resonant case:* $r_0 = 1$

Before proceeding to the study of the case with $r_0 = 1$ let us consider in more detail dispersion properties of axisymmetric waves. First and foremost let us look at the phase velocity $c(k) = \mathrm{Im}\,\omega_1(k)/k$ (figure 12). The phase speed is almost constant ($c \approx -3$) for a wide range of wavenumbers $1 < k < 2.5$ which corresponds to the most unstable waves. The condition of subharmonic resonance $c(k) = c(\frac{1}{2}k)$ is valid for $k = k_s \approx 2.2 \approx k_0^{\max}$. The stable region has practically disappeared (figure 1*b*): the neutral wavenumber $k \approx 0.1$ (compare with figure 1*a* for $r_0 = 3$). As a result the weakly nonlinear effects appear as early as $t = 3$: the local maximum is clearly seen in figure 13(*a*) at $k = k_s \approx 2.2$ – this is the generation of the second harmonic with respect to the subharmonic with $k = \frac{1}{2}k_s$. One can see that in this case only the fundamental wave ($k = k_s$) is greatly amplified (although the subharmonic is also fed, but only slightly), while in the classic case of subharmonic interaction only the subharmonic is greatly fed. As a result of this interaction, at time $t = 4$ the fundamental wave with $k = k_s$ reaches values of amplitudes exceeding those for the linear case by 2–3 times (figure 14*a*). Simultaneously the synchronized spectrum filling takes place (as

$$c(k_1 + k_2) \approx c(k_1) \approx c(k_2)$$

for $1 < k_1, k_2 < 2.5$), the Fourier amplitude $|\bar{r}_w|$ decaying monotonically as $k \to \infty$ (figures 14*a*, 15*a*). The spectrum is filled very rapidly, so the numerical simulation must be stopped at $t = 4.2$ (compare with the case $r_0 = 3$, when we could compute up to $t = 5.5$).

The synchronized interactions lead to the formation of 'spike' (figure 15*b*). The spike amplitude grows very rapidly and its lengthscale decreases. The spike moves with a velocity which is close to the phase velocity of the most unstable waves, $c \approx 3$, which is explained by the synchronized mechanism of its development. The spike's formation is essentially nonlinear, while the wave packet, spreading in front of it (with the group velocity $U = -\partial\,\mathrm{Im}\,\omega_1/\partial k = 4.5$, see for example, Ryzhov & Terent'ev 1986) remains linear in its nature (figure 14*b*).

It is most likely to suppose that the structure of this spike is described by some singular solution of the triple-deck theory. Such singular structures were proposed by Smith (1988), who concluded that a singularity can occur at finite time in any unsteady

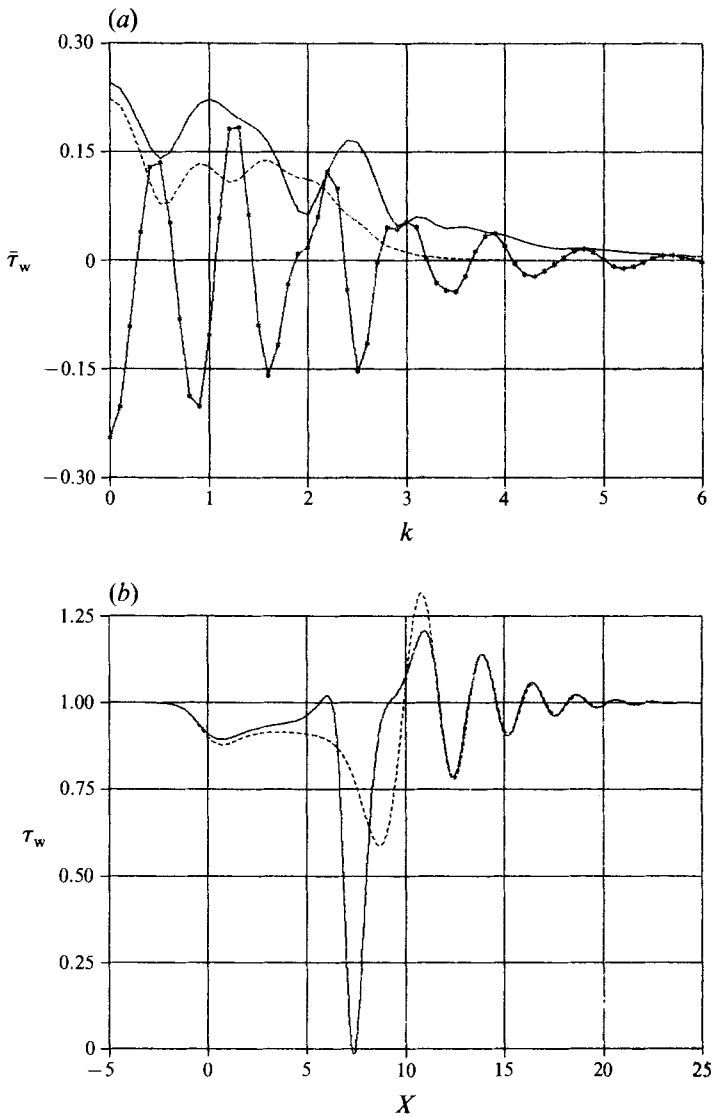

FIGURE 13. (*a*) Spectral distributions at $t = 3$ ($r_0 = 1$): *–*–*–, $\mathrm{Re}\,\bar{\tau}_w(k)$; ——, amplitude $|\bar{\tau}_w|$; ----, $|\bar{\tau}_w|$ for linear case. (*b*) Surface stress $\tau_w(X)$ at $t = 3$ ($r_0 = 1$): ——, fully nonlinear; ----, linear case.

interacting boundary-layer formulation. Unfortunately, the pseudo-spectral method used in the present paper (as any conventional Euler method) exhibits severe difficulty in accurately evaluating the intense variations in flow field and fails to provide results for times immediately prior to the appearance of a singularity. The Lagrangian method is more suitable for the computation of unsteady boundary-layer flows that develop an eruptive character. This method was recently applied by Peridier, Smith & Walker (1991*b*) in the interacting boundary-layer formulation. Their results appear to confirm quantitatively that the singularity encountered is that described by Smith (1988) in what was termed 'moderate break-up' of the interacting boundary-layer formulation. The present results are very similar to those of Peridier *et al.* (1991*b*) in the structure of the singularity that forms (the form of sharp spike, three-tier structure of velocity profiles near the point of breakup, etc.). Of course, the present computations are too

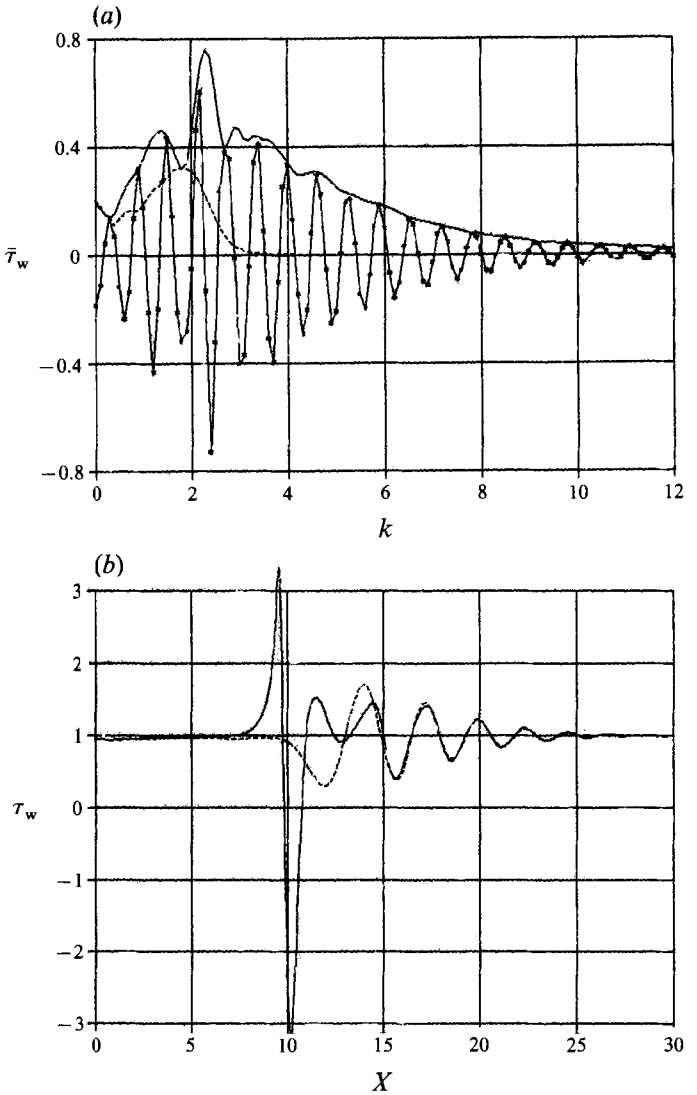

FIGURE 14. Same as figure 13 but at $t = 4$.

inaccurate for resolving which singular structure is formed, but the tendency to its formation is clearly seen.

Anyhow, the present results point to the formation of a concentrated vortex which may be a source of a turbulent spot, as was proposed by Smith *et al.* (1990).

4.1.3. *Far downstream location of disturbances*

Next we pursue an investigation of the problem of the development of disturbances located far downstream. Computational results for $r_0 = \frac{1}{4}$ are presented in figure 16. Here a spike is also formed, and the nature of its formation is resonant. To see this nature, we now use an analytical approach to the problem. In the far downstream limit $r_0 \to 0$ from (2.3*c*) it is easy to obtain that

$$\frac{\bar{p}}{\bar{A}} \equiv \lambda_0(k) = \frac{2}{r_0} + \tfrac{1}{2} r_0 k^2 + O(k^4 r_0^3), \tag{4.2}$$

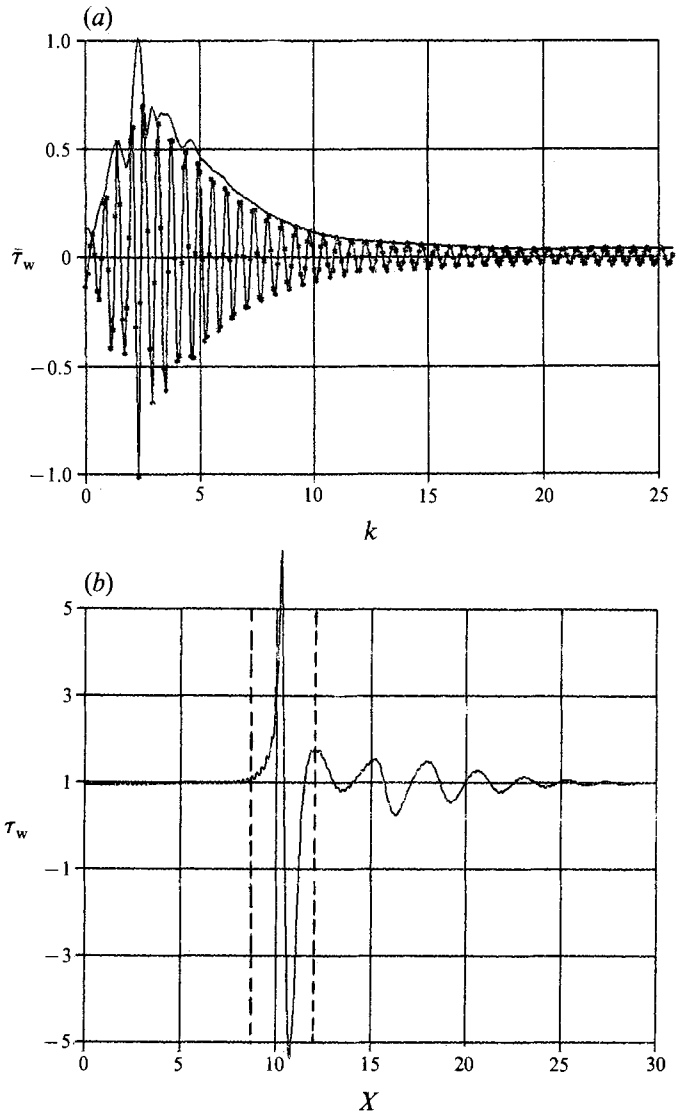

FIGURE 15. Same as figure 13 but at $t = 4.2$.

so
$$\omega_1 = -ik\left(\frac{2}{r_0} + \tfrac{1}{2}r_0 k^2\right) + \tfrac{1}{2}(r_0 k)^{\frac{1}{2}} + O(r_0^{\frac{5}{2}}) \tag{4.3}$$
for $r_0^3 \ll k \ll 1/r_0$.

Hence the phase speed $c_0 = -\operatorname{Im}\omega_1(k)/k \approx 2/r_0$ (i.e. approximately constant) for most waves, and disturbance development takes a synchronized character. Further, growth rates $\operatorname{Re}\omega_1(k)$ fall down decreasing r_0 (see (4.3)), so the process of singularity formation becomes prolonged (figure 16): the spike appears only at $t = 6.5$ and the computation may be continued up to $t = 7$.

One can see here the solitary character of the development of the region with $\tau_w < 1$ (figure 16): distributions of τ_w are almost the same. Here the amplitude growth is connected with the weak instability of the flow. For this case a weakly nonlinear theory in the spirit of Smith (1986) may be constructed. But instead of this we consider another ('far') limit, when instability disappears completely.

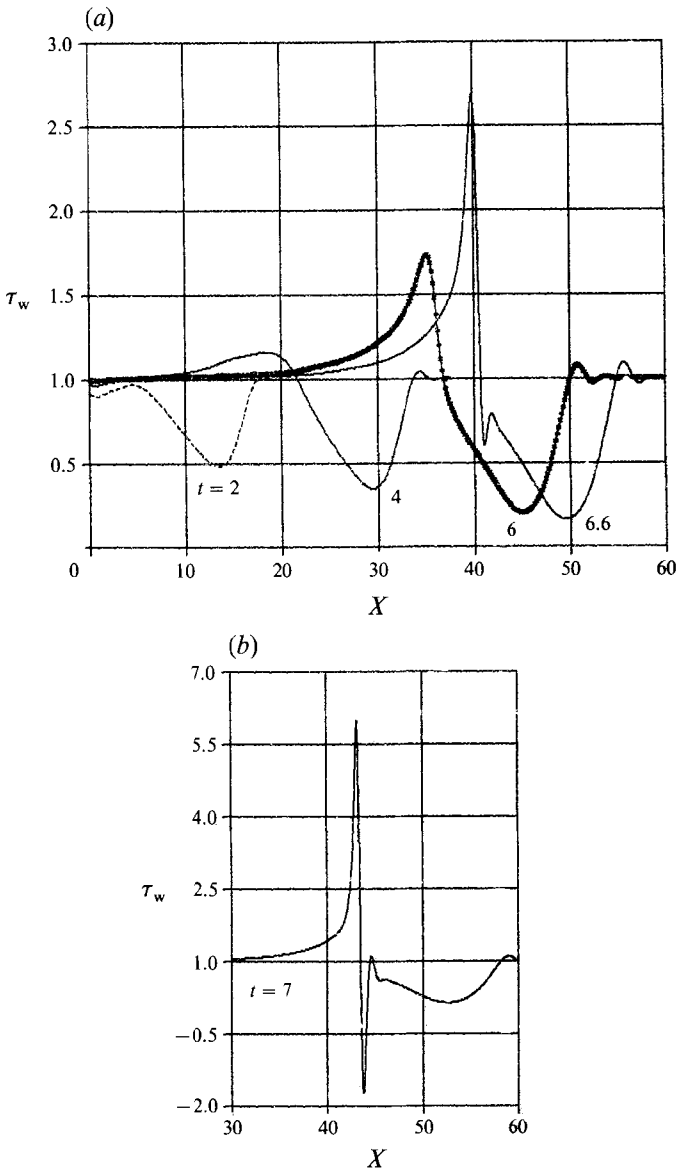

FIGURE 16. Surface stress $\tau_w(X)$ for $r_0 = \frac{1}{4}$ at various times t: (*a*) smooth evolution; (*b*) spike formation.

4.2. *High-frequency/large-amplitude disturbances*

Following to Zhuk & Popov (1989*a*) we set

$$X = \chi^{-1}\tilde{X}, \quad t = \chi^{-2}\tilde{t}, \quad A = \chi\tilde{A}, \quad P = \chi^2\tilde{P}, \quad U = \chi\tilde{U}, \quad V = \chi^3\tilde{V}, \quad Y = \chi\tilde{Y}$$

and take the limit $\chi \to \infty$ in the system (2.2). It is easy to see that the solution of the inviscid problem is thus obtained

$$\tilde{U} = \tilde{Y} + \tilde{A}, \quad \tilde{V} = -\tilde{Y}\frac{\partial\tilde{A}}{\partial\tilde{X}} - \frac{\partial\tilde{A}}{\partial\tilde{t}} - \tilde{A}\frac{\partial\tilde{A}}{\partial\tilde{X}} - \frac{\partial\tilde{P}}{\partial\tilde{X}}. \tag{4.4}$$

The pressure-displacement law (2.3) in new variables is

$$\tilde{P} = \mathscr{L}_0(\tilde{A}), \quad \lambda_0 = \tilde{k} I_0(\tilde{k}\chi r_0)/I_0'(\tilde{k}\chi r_0). \tag{4.5}$$

Choosing the general case $\chi = r_0^{-1}$ and bearing in mind the wall condition $\tilde{V}(\tilde{Y}=0) = \tilde{V}_0$ we finally get the system (tildes are omitted)

$$\frac{\partial A}{\partial t} + A\frac{\partial A}{\partial X} = -\frac{\partial P}{\partial X} - V_0(t, X), \tag{4.6a}$$

$$P = \mathscr{L}_0(A), \quad \mathscr{L}_0(E_0) = \lambda_0(k)E_0, \quad E_0 = \exp(\mathrm{i}kX), \tag{4.6b}$$

$$\lambda_0 = kI_0(k)/I_0'(k), \tag{4.6c}$$

which governs the spreading of high-frequency/large-amplitude lower-branch disturbances.

The no-slip condition on the wall may be satisfied by introduction of a viscous wall sublayer of thickness $\Delta Y = O(\chi^{-1})$. The motion in this sublayer is governed by the classical system of Prandtl equations with prescribed pressure which will be known after solving (4.6). Whether this problem with prescribed pressure gradient has a solution at any time or really terminates in a finite-time singularity is the problem that calls for further investigation. Very often boundary-layer solutions break down in a finite-time singularity, see for example, Peridier *et al.* (1991*a*, *b*) and references therein. But there are cases when the solution does exist. For example, Zhuk (1992) has shown that a consistent boundary layer can be fitted beneath the Benjamin–Ono solitary train.

5. Solitons

5.1. *Large-sized, short-scaled disturbances* ($\Delta \gg R^{-\frac{1}{5}}$)

The system (4.6) can be obtained directly from the original Navier–Stokes equations. Setting $\Delta \gg R^{-\frac{1}{5}}$ (see (2.3)) leads to an inviscid problem having solution (4.4) which immediately gives rise to the system (4.6). Such large-sized, short-scaled (in comparison with standard triple-deck scaling) inviscid disturbances was first considered by Zhuk & Ryzhov (1982) and more recently by Smith & Burggraf (1985), who reasoned that a subsequent stage of the instability process (after the stage of linear amplification) is the 'Euler stage' governed by an equation of type (4.6*a*) which for the problem of an incompressible boundary layer on a flat plate coincides with the classic Benjamin–Ono equation. This idea was developed by Rothmayer & Smith (1987) and more recently by Ryzhov (1990) in connection with experimentally observed soliton-like structures (Borodulin & Kachanov 1990; Kachanov 1991*a*, *b*) in the *K*-regime of boundary-layer transition.

The fundamental feature of the Benjamin–Ono equation is that it has solutions in the form of solitons. A similar feature is inherent in the homogeneous system (4.6) which will be studied in the next subsection.

5.2. *Homogeneous problem*

First of all, we prove that the homogeneous system (4.6), i.e.

$$\frac{\partial A}{\partial t} + A\frac{\partial A}{\partial X} = -\frac{\partial P}{\partial X}, \quad P = \mathscr{L}_0(A), \quad \lambda_0 = k\frac{I_0(k)}{I_0'(k)}, \tag{5.1a–c}$$

is conservative. After multiplication of (5.1*a*) by $A(t, X)$ and integration of the result with respect to X from $-\infty$ to $+\infty$ (suggesting $|A| \to 0$ as $X \to \pm\infty$) we obtain

$$\frac{1}{2}\frac{\partial}{\partial t}\langle A^2\rangle = -\left\langle A\frac{\partial P}{\partial X}\right\rangle, \tag{5.2}$$

where $\langle B\rangle = \int_{-\infty}^{\infty} B\,\mathrm{d}X$. Using the convolution integral

$$\langle AB\rangle = 2\pi\int_{-\infty}^{\infty} \bar{A}(k)\,\bar{B}(-k)\,\mathrm{d}k$$

immediately leads to

$$\left\langle A\frac{\partial P}{\partial X}\right\rangle = 2\pi\int_{-\infty}^{\infty} \mathrm{i}k\lambda_0(k)\,\bar{A}(k)\,\bar{A}(-k)\,\mathrm{d}k = 0$$

because the integrant is an odd function ($\lambda_0(k)$ is an even function and $\bar{A}(k)\,\bar{A}(-k)$ is always even). Thus $\langle A^2\rangle = \text{const}$, that is the system preserves its energy in time.

It is well known that competition between dispersion and nonlinearity may lead to the formation of solitons, as this is the case for the Benjamin–Ono equation. Therefore one can expect that the (5.1) has solitary solutions as well.

5.2.1. *Long-wave limit: Korteweg–de Vries equation*

We start to study solitons using limiting cases. In the long-wave limit $k \to 0$ the interaction law (5.1*b*) reduces to

$$\bar{P}/\bar{A} \equiv \lambda_0(k) = 2 + \tfrac{1}{2}k^2 + O(k^4) \quad \text{as} \quad k \to 0, \tag{5.3a}$$

or

$$P = 2A - \tfrac{1}{2}\partial^2 A/\partial X^2. \tag{5.3b}$$

Hence (5.1*a*) takes the form

$$\frac{\partial A}{\partial t} + A\frac{\partial A}{\partial X} = -2\frac{\partial A}{\partial X} + \frac{1}{2}\frac{\partial^3 A}{\partial X^3}. \tag{5.4}$$

By using

$$A = -\tfrac{1}{2}\tilde{A}, \quad X = -\sqrt{6}\tilde{X} + 2t, \quad t = 12\sqrt{6}\tilde{t} \tag{5.5}$$

it transforms into the classic Korteweg–de Vries equation which has the well-known one-soliton solution. In original variables this solution becomes

$$A = -A_0\,\mathrm{sech}^2\left((A_0/6)^{\frac{1}{2}}[X - ct]\right), \tag{5.6a}$$

$$c = c(A_0) = 2 - A_0/3, \tag{5.6b}$$

where amplitude $A_0 = \text{const} > 0$. The region of applicability of approximation (5.6) to the original problem (5.1) is restricted to small A_0 because (5.4) was obtained in the long-wave limit and hence the spatial size $|A_0/6|^{\frac{1}{2}} \ll 1$.

The formula (5.6*b*) shows that the velocity of a soliton cannot exceed the value $c(A_0 = 0) = 2$. This conclusion is valid in the general case and we prove it now without a supposition about the smallness of amplitude A_0. Taking the form of running waves $A = A_v(X - ct)$ and assuming $|A_v(\xi)| \to 0$ as $\xi \to \pm\infty$ after integration we have

$$-cA_v(\xi) + \tfrac{1}{2}A_v^2(\xi) = -P(\xi).$$

The second integration from $-\infty$ to $+\infty$ yields

$$\langle A_v^2\rangle = 2\pi(c\bar{A}_v(0) - \lambda_0(0)\,\bar{A}_v(0)) = (c-2)\langle A_v\rangle. \tag{5.7}$$

The left-hand side of (5.7) is a non-negative quantity, hence $c \leqslant 2$ (computations have revealed the existence of solitons with negative 'mass' $\langle A_v\rangle$ only).

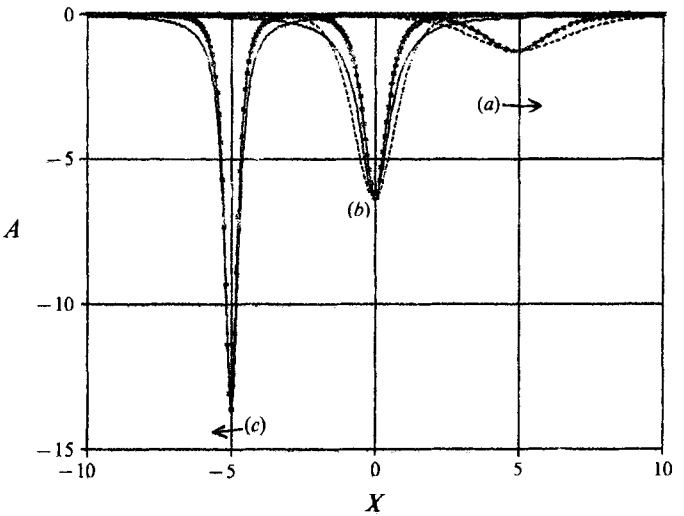

FIGURE 17. Shapes of solitons with amplitude A_0 and phase velocity c: (*a*) $A_0 = 1.25$, $c = 1.7$; (*b*) $A_0 = 6.3$, $c = 0$; (*c*) $A_0 = 13.5$, $c = -2.1$; *−*−*−, original problem (5.1); ----, Korteweg–de Vries approximation; ——, Benjamin–Ono approximation.

Formula (5.6*b*) shows that with an increase of amplitude the soliton moves slower, at some critical value $A_0 = A_* = 6$ stops, and at $A_0 > A_*$ starts to move upstream, its velocity growing linearly with the increase of amplitude. As computations (based on a pseudo-spectral scheme) show, this phenomenon does take place; moreover, the formula (5.6*b*) works well up to $A_0 \approx 10$ (so the critical value $A_* = 6.3$ is close to the prediction $A_* = 6$), although the discrepancy in soliton shape is already seen in figure 17 at $A_0 = 1.25$.

5.2.2. *Short-wave limit: Benjamin–Ono equation*

With the increase of amplitude A_0 the characteristic lengthscale of the soliton decreases, therefore at large A_0 the short-wave asymptote must be involved. Taking the limit $k \to \infty$, we have

$$\bar{p}/\bar{A} \equiv \lambda_0(k) = |k| + \tfrac{1}{2} + O(1/k) \quad \text{as} \quad k \to \infty \tag{5.8}$$

thus obtaining the Benjamin–Ono dispersion: $\omega_0(k) = \mathrm{i}k\lambda_0(k) = \mathrm{i}k|k| + \mathrm{i}k/2$ (the second addendum gives only shift in speed; we can exclude it applying the Galilean transformation). Hence in the short-wave limit (5.1*a*) reduces to 'shifted' Benjamin–Ono equation

$$\frac{\partial A}{\partial t} + A\frac{\partial A}{\partial X} = \frac{1}{\pi}\int_{-\infty}^{\infty} \frac{\partial^2 A/\partial \xi^2}{\xi - X}\,\mathrm{d}\xi - \frac{1}{2}\frac{\partial A}{\partial X}, \tag{5.9}$$

the well-known one-soliton solution of which has the form

$$A = -\frac{A_0}{1 + A_0^2(X - ct)^2/16}, \tag{5.10a}$$

$$c = -A_0/4 + \tfrac{1}{2}. \tag{5.10b}$$

The formula (5.10*b*) is unusable for estimation of the critical value of A_* (it gives $A_* = 2$), but it approximates the shape of a motionless soliton much better than the long-wave analogue (5.6*a*). Much better results are given by (5.10*a*) for the soliton shape at $A_0 = 13.5$ (figure 17), whereas velocity $c \approx -2.9$ given by (5.10*b*) differs

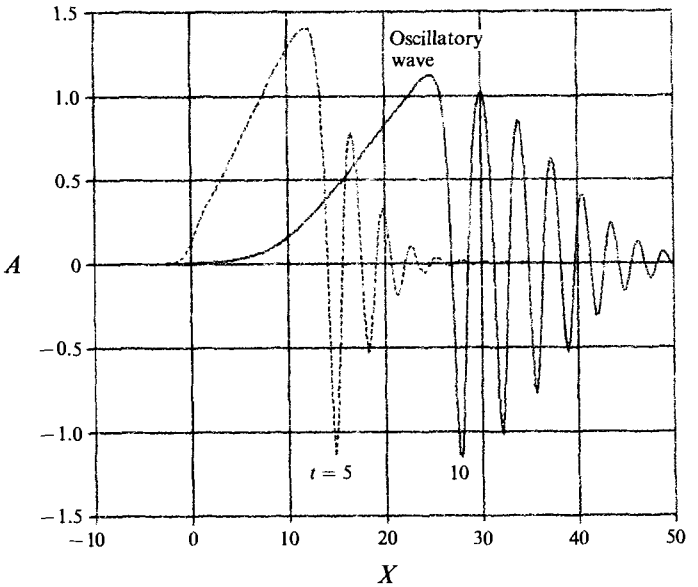

FIGURE 18. Oscillatory wave produced by pulse suction ($H = -7$).

noticeably from the accurate value $c = -2.1$. Thus the long-wave approximation (5.6) gives a good estimation of the soliton velocity and the short-wave one (5.10) of its shape.

Finally, further computations confirm that the solitary waves obtained are solitons, i.e. they reproduce their shapes after interactions.

5.3. *Soliton generation*

Next we shall study the inhomogeneous problem (4.6) with the forcing term V_0 which represents various external sources: humps, injections etc. So we shall study the nonlinear receptivity problem for large-sized short-scaled disturbances. Corresponding inhomogeneous problems in boundary-layer situations have been studied in a number of Russian works: by Zhuk & Popov (1989*a*) and Popov (1992) for a subsonic boundary layer on a flat plate, by Zhuk & Popov (1989*b*) for its supersonic counterpart, and by Zhuk & Popov (1989*b*) for an incompressible jet developing along a wall.

5.3.1. *Disturbances produced by suction*

We start to analyse the problem (4.6) with the most simple (in solution behaviour) case of suction which corresponds to $H < 0$ when choosing a disturbance source in the form

$$V_0 = Hf(t)\,V_{00}(X), \quad V_{00} = \exp(-X^2). \tag{5.11}$$

A pulse source with

$$f = t\exp(-t) \tag{5.12}$$

produces only an oscillatory wave with the amplitude slowly decaying in time (figure 18).

A quasi-stationary source with

$$f = \begin{cases} t, & t \leqslant 1, \\ 1, & t > 1 \end{cases} \tag{5.13}$$

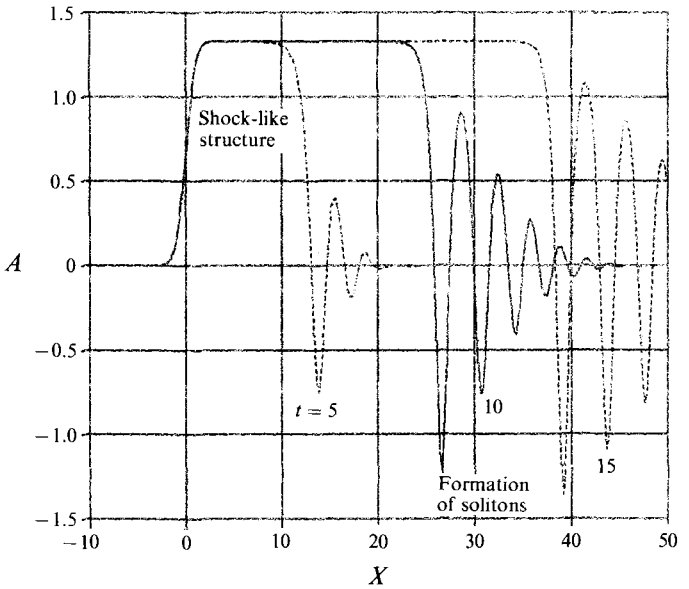

FIGURE 19. Disturbances from quasi-stationary suction ($H = -2$).

forms a shock-like structure (figure 19) which is governed by the equation

$$\tfrac{1}{2}A^2(X) + P(X) = -\int_{-\infty}^{X} V_0(t=\infty, \xi)\,\mathrm{d}\xi. \tag{5.14}$$

In the present case $\langle V_0 \rangle \neq 0$, so $A_\infty = A(\infty) \neq 0$. The quantity A_∞ gives the non-zero background for a spreading oscillatory wave (figure 19). On the tail of this wave where it touches the non-zero background a soliton starts to form. It moves faster than a soliton of the same amplitude spreading on the zero background. It is easy to see by performing the Galilean transformation: so if $A_s(X-ct)$ is a solution of (5.1), then

$$A_\infty + A_s(X-(c+A_\infty)\,t)$$

is also a solution. Later the second soliton starts to form in its turn (figure 19). In the limit $t \to \infty$ its amplitude reaches the value of the first one. Generally at $t = \infty$ the oscillatory wave transforms into a soliton train.

Thus *only stationary* suction produces solitons which can run *only downstream.*

5.3.2. *Soliton generation by blowing*

Blowing brings a negative 'mass' $\langle V_0 \rangle < 0$, thanks to which generation of solitons has already taken place in the regime of a pulse source. A perturbation of the form (5.11) and (5.12) with $H > 0$ generally produces two solitons and a barely distinguishable (on their level) oscillatory wave; for a typical pattern see figure 20.

The non-vanishing influence on the flow by means of blowing leads to the generation of a soliton train (figure 21). Knowing 'mass' $|\langle A_s \rangle|$ and velocity c_s of a single soliton it is easy to estimate both the number of solitons generated up to time t: $N_s \approx \langle V_0 \rangle / \langle A_s \rangle$ and the distance between them in the train: $\Delta X_s = c_s |\langle A_s \rangle / \langle V_{00} \rangle|$.

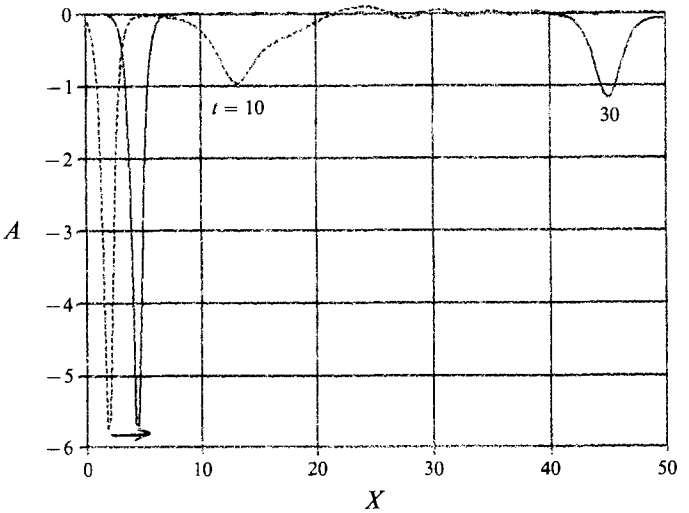

FIGURE 20. Solitons produced by pulse blowing ($H = 7$).

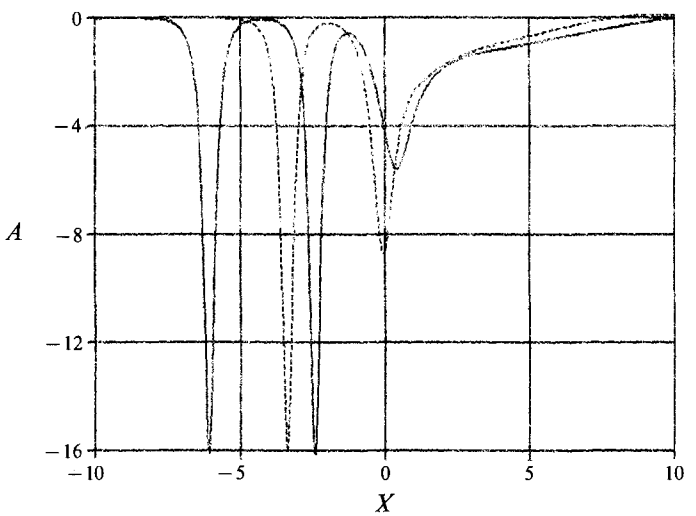

FIGURE 21. Soliton train from quasi-stationary blowing ($H = 5$).

5.3.3. *Disturbances produced by a quasi-stationary hump*

We can consider other sources of disturbances, for example humps on a wall. If the form of the hump is given by the function $F(t, X)$, the problem under consideration remains the same (see, for example, Zhuk & Popov 1989*a*), namely, (4.6) with the function V_0 given by

$$V_0 = -\frac{\partial}{\partial X}\mathscr{L}_0(F). \tag{5.15}$$

Thus the hump affects the flow as a combined suction–blowing with the zero 'mass' $\langle V_0 \rangle$.

It is easy to see that in the case of the hump the stationary solution vanishing at infinity can exist because the right-hand side of (5.14) tends to zero as $X \to \infty$ and thus this equation immediately gives

$$\mathscr{L}_0(A - F) = \tfrac{1}{2}A^2. \tag{5.16}$$

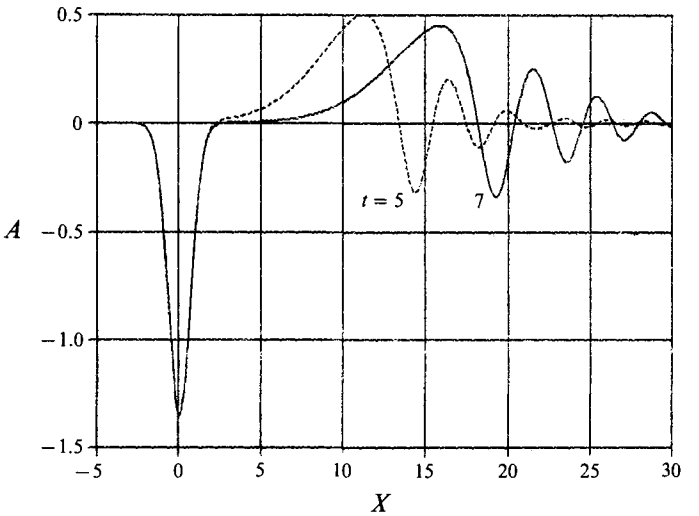

FIGURE 22. Disturbances produced by quasi-stationary hollow ($H = -1$).

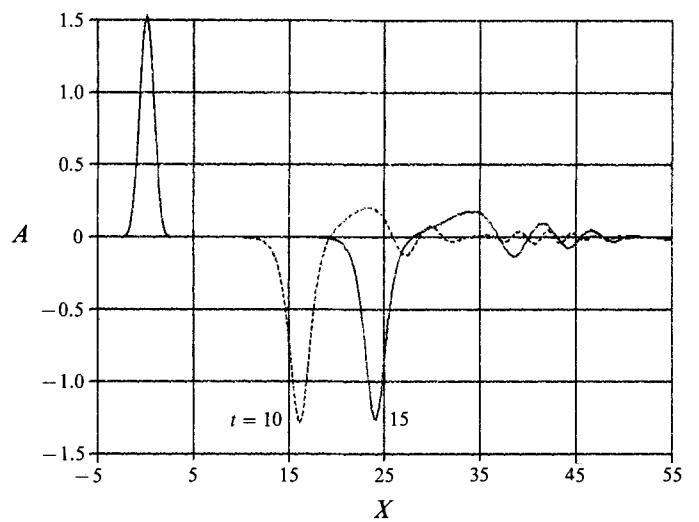

FIGURE 23. Disturbances produced by quasi-stationary hump ($H = 2$).

Integrating (5.16) with respect to X leads to the relation

$$\lambda_0(0)(\langle A\rangle - \langle F\rangle) = \tfrac{1}{2}\langle A^2\rangle,$$

which gives the necessary condition for existence of a stationary solution. Thus classic Benjamin–Ono and Korteweg–de Vries equations admit no stationary solutions (due to $\lambda_0(0) = 0$) whereas such solutions are possible in inlet-flow situations where $\lambda_0(0) \neq 0$.

In fact, computations based on the simplest pseudo-spectral scheme showed that a solution of (5.16) does exist in the range of the hump (hollow) height $H_* < H < \infty$ with $H_* = -1.33$ for $F = F_{00}(X) = H\exp(-X^2)$. Such stationary solutions are clearly seen in figures 22 and 23: they are parts of solutions, centred around $X = 0$. Here the stationary hump produces no stationary upstream or wake effects as is the case in some

range of flow parameters, when $\Delta \sim R^{-\frac{1}{5}}$ (Smith 1976). This can be directly seen from (5.16) because in the far-upstream and far-downstream regions, where $|A|$ is vanishingly small, neglecting of the nonlinear term in (5.16) gives $A \to F$ as $X \to \pm\infty$.

6. Discussion and conclusions

Thus a detailed study of disturbance development, both three-dimensional linear and axisymmetric nonlinear, has been done in the framework of asymptotic triple-deck theory. The linear analysis has shown that resonant wave interactions are possible on the purely axisymmetric disturbances. Numerical computations have confirmed that resonant interactions do take place. They lead to enhanced disturbance growth, producing a sharp spike which represents a concentrated vortex. The amplitude of the spike grows very rapidly, so the boundary-layer solution seems to develop a finite-time singularity.

Relatively high-frequency/large-amplitude disturbances (with respect to lower-branch scaling) have been considered as well. They are predominantly inviscid, i.e. they are governed by inviscid equations (although finally the Prandtl problem for boundary-layer equations must be solved). The characteristic feature of this inviscid problem is that it has solutions in the form of solitons which can run both upstream and downstream depending on their amplitude. These solitary solutions are exceptionally intriguing in connection with recent controlled experiments by Borodulin & Kachanov (1990) and Kachanov (1991 *a*, *b*) in which soliton-like structures were observed in the *K*-regime of laminar–turbulent transition in the boundary layer on a flat plate.

Strictly speaking, the present analysis reveals *limiting* properties of disturbed flow, as the Reynolds number tends to infinity. So what will be the case in the practical situation of high but finite Reynolds number, high but finite frequency of perturbation? We can suggest that in the initial linear stage, where the linearly most unstable waves are of primary importance, lower-branch disturbances must predominate. Then they must be amplified through the powerful mechanism of resonant interactions, which play the leading role in both *K*- and *N*-regimes of flat-plate boundary-layer transition (Kachanov & Levchenko 1982; Borodulin & Kachanov 1989). The amplitude of disturbances grows very rapidly, provoking transition to the fully nonlinear stage. This stage of relatively high-amplitude disturbances must be governed, it seems, by the inviscid system of equations studied in § 5. (Such a transition from one scale to another was proposed and developed in a number of early papers dealing with high-Reynolds-number instability, see Smith & Burggraf 1985, Rothmayer & Smith 1987, Smith *et al.* 1990, Ryzhov 1990.) Thus solitons must be formed. In summary, it is exactly the scenario of the *K*-regime of transition in the boundary layer on a flat plate: the linear amplification and selection – resonant interactions – the formation of solitons. So we have every reason to believe that such a scenario may take place in laminar–turbulent transition in inlet flows (resonant interactions and solitons are inherent features for inlet channel flow as well, see Savenkov 1992).

The author would like to thank Dr V. V. Kozlov for constructive criticism, Professor O. S. Ryzhov, Dr Yu. S. Kachanov and Dr V. I. Zhuk for helpful discussions. The author wishes particularly to acknowledge his thanks to Professor F. T. Smith, Dr S. J. Cowley and an anonymous referee for their comments and suggestions which have led to substantial improvement of the paper. The author is very appreciative to Mrs A. I. Derzhavina for help with the English.

REFERENCES

BOGDANOVA, E. V. 1982 On the free oscillations of viscous incompressible fluid in a semi-infinite circular pipe. *Dokl. Akad. Nauk. USSR* **263**, 829–833 (in Russian).

BOGDANOVA, E. V. & RYZHOV, O. S. 1983 On free oscillations of viscous incompressible fluid in a semi-infinite channel. *Prikl. Matem. Mekh.* **47**, 64–72.

BORODULIN, V. I. & KACHANOV, YU. S. 1989 The series of harmonic and parametric resonances in the *K*-regime of breakdown of laminar boundary layer. *Modelir. v. Mekh., Siberian Div. Akad. Sci. USSR*, ITPM **3(20)**, No. 2 (in Russian).

BORODULIN, V. I. & KACHANOV, YU. S. 1990 Experimental study of soliton-like coherent structures in boundary layer. In *Proc. 19th Session Scientific and Methodological Seminar on Ship Hydrodynamics, 1–6 Oct. Varna, Bulgaria*, vol. 2, pp. 99-1–99-10. Bulgarian Ship Hydrodynamics Centre.

BURGGRAF, O. R. & DUCK, P. W. 1982 Spectral computation of triple-deck flow. In *Numerical and Physical Aspects of Aerodynamic Flows* (ed. T. Cebeci), pp. 145–158. Academic.

CRAIK, A. D. D. 1971 Nonlinear resonant instability in boundary layers. *J. Fluid Mech.* **50**, 393–413.

DUCK, P. W. 1985 Laminar flow over unsteady humps: the formation of waves. *J. Fluid Mech.* **160**, 465–498.

DUCK, P. W. 1987 Unsteady triple-deck flows leading to instabilities. In *Proc. IUTAM Symp. on Boundary-Layer Separation*, pp. 297–312. Springer.

DUCK, P. W. 1990 Triple-deck flow over unsteady surface disturbances: the three-dimensional development of Tollmien–Schlichting waves. *Computers Fluids.* **18**, 1–34.

GOLDSTEIN, M. E. & CHOI, S.-W. 1989 Nonlinear evolution of interacting oblique waves on two-dimensional shear layers. *J. Fluid Mech.* **207**, 97–120.

GOLDSTEIN, M. E. & HULTGREN, L. S. 1989 Boundary-layer receptivity to long-wave free-stream disturbances. *Ann. Rev. Fluid Mech.* **21**, 137–166.

GOLDSTEIN, M. E. & LEIB, S. J. 1989 Nonlinear evolution of oblique waves on compressible shear layers. *J. Fluid Mech.* **207**, 73–96.

HUANG, L. M. & CHEN, T. S. 1974 Stability of developing pipe flow subjected to non-axisymmetric disturbances. *J. Fluid Mech.* **63**, 183–193.

KACHANOV, YU. S. 1987 On the resonant nature of the breakdown of a laminar boundary layer. *J. Fluid Mech.* **184**, 43–74.

KACHANOV, YU. S. 1991*a* Resonant-soliton nature of boundary layer transition. *Russian J. Theor. Appl. Mech.* 1 (2), 79–94.

KACHANOV, YU. S. 1991*b* The mechanism of formation and breakdown of soliton-like structures in boundary layer. In *Advances in Turbulence* (ed. A. V. Johansson & P. H. Alfredsson), pp. 42–51. Springer.

KACHANOV, YU. S. & LEVCHENKO, V. YA. 1982 The resonant interaction of disturbances at laminar – turbulent transition in a boundary layer. Preprint 10-82, Novosibirsk, ITPM SO AN SSSR (in Russian).

KACHANOV, YU. S. & LEVCHENKO, V. YA. 1984 The resonant interaction of disturbances at laminar turbulent transition in a boundary layer. *J. Fluid Mech.* **138**, 209–247.

KLEBANOFF, P. S., TIDSTROM, K. D. & SARGENT, L. M. 1962 The three-dimensional nature of boundary-layer instability. *J. Fluid Mech.* **12**, 1–34.

KOZLOV, V. V. & RYZHOV, O. S. 1990 Receptivity of boundary layers: asymptotic theory and experiment. *Proc. R. Soc. Lond.* A **429**, 341–373.

MESSITER, A. F. 1970 Boundary layer flow near the trailing edge of a flat plate. *SIAM J. Appl. Maths* **18**, 241–257.

NEILAND, V. YA. 1969 Towards the theory of separation of the laminar boundary layer in a supersonic flow. *Izv. Akad. Nauk USSR, Mekh. Zhidk. i Gaza* **4**, 53–57 (in Russian).

PERIDIER, V. J., SMITH, F. T. & WALKER, J. D. A. 1992*a* Vortex-induced boundary-layer separation. Part 1. The unsteady limit problem $Re \to \infty$. *J. Fluid Mech.* **232**, 99–131.

PERIDIER, V. J., SMITH, F. T. & WALKER, J. D. A. 1992*b* Vortex-induced boundary-layer separation. Part 2. Unsteady interacting boundary-layer theory. *J. Fluid Mech.* **232**, 133–165.

POPOV, S. P. 1992 On soliton perturbations excited by an oscillator in a boundary layer. *Comput. Maths Mech. Phys.* **32** (1), 61–69.

REYNOLDS, O. 1883 Experimental investigation of the circumstances which determine whether the motion of water shall be direct or sinuous and the law of resistance in parallel channels. *Phil. Trans. R. Soc.* **174**, 935–982.

ROTHMAYER, A. P. & SMITH, F. T. 1987 Strongly nonlinear wave-packets in boundary layers. *Trans. ASME* I: *J. Fluids Engng* June, 67.

RYZHOV, O. S. 1990 On the formation of organized vortex structures from unstable oscillations in a boundary layer. *Zh. Vich. Matem. Mat. Fiz.* **30**, 1804–1814 (in Russian).

RYZHOV, O. S. & SAVENKOV, I. V. 1989 Asymptotic approach to hydrodynamic stability theory. *Mathematical Simulation* **1** (4), 61–86 (in Russian).

RYZHOV, O. S. & SAVENKOV, I. V. 1992 On the nonlinear stage of perturbation growth in boundary layer. In *Modern Problems in Computational Aerodynamics* (ed. A. A. Dorodnicyn & P. I. Chushkin), pp. 81–92. Mir Publishers & CRC Press.

RYZHOV, O. S. & TERENT'EV, E. D. 1986 On the transition regime, which characterizes the start-up process of vibrator oscillations in a subsonic boundary layer on a flat plate. *Prikl. Matem. Mekh.* **50**, 974–986 (in Russian).

SARPKAYA, T. 1975 A note on the stability of developing laminar pipe flow subjected to axisymmetric and non-axisymmetric disturbances. *J. Fluid Mech.* **68**, 345–351.

SAVENKOV, I. V. 1992 The resonant amplification of two-dimensional disturbances in a semi-infinite channel. *Zh. Vich. Matem. Mat. Fiz.* **32**, 1332–1339 (in Russian).

SMITH, F. T. 1976 On entry-flow effects in bifurcating, blocked or constricted tubes. *J. Fluid Mech.* **78**, 709–736.

SMITH, F. T. 1979 On the non-parallel flow stability of the Blasius boundary layer. *Proc. R. Soc. Lond.* A **366**, 91–109.

SMITH, F. T. 1986 Two-dimensional disturbance travel, growth and spreading in boundary layers. *J. Fluid Mech.* **169**, 353–377.

SMITH, F. T. 1988 Finite-time break-up can occur in any unsteady interacting boundary layer. *Mathematika* **35**, 256–273.

SMITH, F. T. & BODONYI, R. J. 1980 On the stability of the developing flow in a channel or circular pipe. *Q. J. Mech. Appl. Maths* **33**, 293–320.

SMITH, F. T. & BODONYI, R. J. 1982 Amplitude-dependent neutral modes in the Hagen–Poiseuille flow through a circular pipe. *Proc. R. Soc. Lond.* A **384**, 463–489.

SMITH, F. T. & BURGGRAF, O. R. 1985 On the development of large-sized short-scaled disturbances in boundary layers. *Proc. R. Soc. Lond.* A **399**, 25–55.

SMITH, F. T., DOORLY, D. J. & ROTHMAYER, A. P. 1990 On displacement-thickness, wall-layer and mid-flow scales in turbulent boundary layers, and slugs of vorticity in channel and pipe flows. *Proc. R. Soc. Lond.* A **428**, 255–281.

SMITH, F. T. & STEWART, P. A. 1987 The resonant-triad nonlinear interaction in boundary-layer transition. *J. Fluid Mech.* **179**, 227–252.

STEWARTSON, K. 1969 On the flow near the trailing edge of a flat plate – II. *Mathematika* **16**, 106–121.

TATSUMI, T. 1952 Stability of the laminar inlet-flow prior to the formation of Poiseuille regime. *J. Phys. Soc. Japan* **7**, 489.

WYGNANSKI, I. J. & CHAMPAGNE, F. H. 1973 On transition in a pipe. Part 1. The origin of puffs and slugs and the flow in a turbulent slug. *J. Fluid Mech.* **59**, 281–335.

ZHUK, V. I. 1993 On the nonlinear disturbances in a boundary layer with self-induced pressure on a flat plate in transonic flow. *Prikl. Matem. Mekh.* (to appear) (in Russian).

ZHUK, V. I. & POPOV, S. P. 1989*a* On the solutions of inhomogeneous Benjamin–Ono equation. *Zh. Vich. Matem. Mat. Fiz.* **29**, 1852–1862 (in Russian).

ZHUK, V. I. & POPOV, S. P. 1989*b* On the nonlinear development of longwave inviscid disturbances in a boundary layer. *Zh. Prikl. Makh. Tekhn. Fiz.* **3**, 101–108 (in Russian).

ZHUK, V. I. & RYZHOV, O. S. 1980 Free interaction and stability of an incompressible boundary layer. *Dokl. Akad. Nauk. USSR* **253**, 1326–1329 (in Russian).

ZHUK, V. I. & RYZHOV, O. S. 1982 On the locally inviscid disturbances in a boundary layer with self-induced pressure. *Dokl. Akad. Nauk. USSR* **263**, 56–59 (in Russian).